



Drought effects on leaf fall, leaf flushing and stem growth in Neotropical forest; reconciling remote sensing data and field observations

5 Thomas Janssen¹, Ype van der Velde¹, Florian Hofhansl², Sebastiaan Luyssaert³, Kim Naudts¹, Bart Driessen⁴, Katrin Fleischer⁵ and Han Dolman¹

¹ Department of Earth Sciences, Vrije Universiteit Amsterdam, Amsterdam, the Netherlands

² International Institute for Applied Systems Analysis (IIASA), Laxenburg, Austria

³ Department of Ecological Sciences, Vrije Universiteit Amsterdam, Amsterdam, the Netherlands

10 ⁴ Department of Computer Science, Universidad de Alcalá de Henares, Madrid, Spain

⁵ Department of Biogeochemical Signals, Max Planck Institute for Biogeochemistry, Jena, Germany

Correspondence to: Thomas Janssen (t.a.j.janssen@vu.nl)

15 **Abstract.**

Large amounts of carbon flow through tropical ecosystems every year, from which a part is sequestered in biomass through tree growth. However, the effects of ongoing warming and drying on tree growth and carbon sequestration in tropical forest is still highly uncertain. Field observations are sparse and limited to a few sites while remote sensing analysis shows diverging growth responses to past droughts that cannot be interpreted with confidence. To reconcile data from field observations and remote sensing, we collated in situ measurements of stem growth and leaf litterfall from inventory plots across the Neotropics. This data was used to train two machine learning models and to evaluate model performance on reproducing stem growth and litterfall rates. The models utilized multiple climatological variables and other geospatial datasets as explanatory variables. The output consisted of monthly estimates of leaf litterfall ($R^2 = 0.67$, $NRMSE = 9.5\%$) and stem growth ($R^2 = 0.51$, $NRMSE = 11.2\%$) across the neotropics from 1982 to 2019 at a high spatial resolution (0.1°). Modelled time series allowed to assess the impacts of the 2005 and 2015 droughts in the Amazon basin on regional scales. Both droughts were estimated to have caused widespread declines in stem growth ($-0.6\sigma \sim -1.8\sigma$), coinciding with enhanced leaf fall ($+0.7\sigma \sim +0.9\sigma$). Regions in the Amazon basin that flushed leaves at the onset of both droughts ($+1.1\sigma \sim +1.9\sigma$), showed positive anomalies in remotely sensed enhanced vegetation index, while sun-induced fluorescence and vegetation optical depth were reduced. The previously observed counterintuitive response of canopy green-up during drought in the Amazon basin detected by many remote sensing analyses can therefore be explained by enhanced leaf flushing at the onset of a drought. The long-term estimates of leaf litterfall and stem growth point to a decline of stem growth and a simultaneous but weaker increase in leaf litterfall in the Amazon basin since 1982 that is not observed in long-term inventory plots. These trends are associated with increased warming and drying of the Amazonian climate.



1 Introduction

35 Tropical forests, in particular in the Amazon basin, contribute substantially (~25%) to the terrestrial carbon sink (Brienen et al., 2015; Pan et al., 2011). The Amazon forest alone currently stores an estimated 100 to 115 Pg of carbon in living biomass and intact forests have taken up an additional net 0.43 Pg of carbon each year through tree stem growth since the 1980's (Feldpausch et al., 2012; Phillips et al., 2017). It thereby counteracts the impact of deforestation and fossil fuel emissions on the atmospheric CO₂ growth rate and mitigates global climate change (Phillips et al., 2017). Most land surface models project
40 that the Amazon carbon sink will be sustained throughout the 21st century, mainly driven by the positive effect of elevated atmospheric CO₂ on plant growth (i.e. CO₂ fertilization) (Holm et al., 2020; Rammig et al., 2010). Also forest plot inventory data suggests a persistent carbon sink in intact Neotropical forests (Phillips et al., 2008) although the sink strength (i.e. the rate of net carbon uptake) has been declining since the start of the 21st century (Brienen et al., 2015; Hubau et al., 2020). The decline of the carbon sink strength is mainly driven by increased tree mortality while tree growth remained relatively stable
45 (Brienen et al., 2015). This suggests that the positive effect of elevated atmospheric CO₂ on plant photosynthesis and growth may increasingly be cancelled out by other limiting factors, such as nutrient availability (Fleischer et al., 2019; Hofhansl et al., 2016; Lapola et al., 2009). Additionally, the Amazon region is experiencing a decline of dry season precipitation, more frequent episodic droughts and increasing regional air temperatures (Cox et al., 2008; Fu et al., 2013; Janssen et al., 2020a; Jiménez-Muñoz et al., 2016). In light of these observed changes in regional climate and forest functioning, it is highly uncertain whether
50 intact Neotropical forest will continue to act as a carbon sink in the future or will become a net source of CO₂ that will amplify global climate change (Boisier et al., 2015; Fu et al., 2013; Janssen et al., 2020a; Malhi et al., 2009b; Marengo et al., 2010).

1.1 How sensitive is tree growth to drought in Neotropical forests?

Past responses of the Amazon forest productivity to droughts have been studied using satellite remote sensing analyses and field observations but sometimes with conflicting results. For example, many field observations show clear reductions in tree
55 stem growth during drought (Feldpausch et al., 2016; Hofhansl et al., 2014; Rifai et al., 2018) while others found no reductions in stem growth during a drought (Doughty et al., 2015a; Phillips et al., 2009). Remote sensing studies complemented field observations and provided useful insights into the responses of forest productivity and aboveground biomass to drought over time on regional and global scales (e.g. Liu et al., 2018b; Saleska et al., 2007). However, as remote sensing techniques measure electromagnetic radiation, it is notoriously difficult to interpret an observed drought response in remote sensing data and
60 translate this response into a quantifiable change in growth or ecosystem carbon uptake (Mitchard et al., 2009a, 2009b). Furthermore, different remote sensing sensors sometimes point to contrasting responses of forest productivity to drought and seem to be deviating from ground observations (Anderson et al., 2010).

The discrepancy between drought responses observed in remote sensing products can partly be explained by the range of the
65 electromagnetic spectrum that the sensors utilize, so that the retrieved signal is sensitive to different vegetation properties.



Multispectral sensors that utilize red and near-infrared bands in the spectrum are sensitive to vegetation greenness and consistently show canopy green-up during and just after drought (Gonçalves et al., 2020; Lee et al., 2013; Saleska et al., 2007; Yang et al., 2018). However, other evidence from remote sensing analyses seem to contradict this so-called Amazon green-up during drought (Anderson et al., 2018; Xu et al., 2011). Firstly, sun-induced fluorescence (SIF), measured with hyperspectral sensors and regarded a good proxy of canopy photosynthesis, is generally found to decrease during drought (Koren et al., 2018; Lee et al., 2013; Yang et al., 2018). Secondly, remotely sensed passive and active microwave data show clear negative anomalies in vegetation optical depth (VOD) and radar backscatter in response to drought in the Amazon basin, both are considered sensitive to vegetation water content and biomass (Frolking et al., 2011, 2017; Liu et al., 2018b; Saatchi et al., 2013). For example, monthly observations of remotely sensed radar backscatter showed clear negative anomalies during the 2015 drought in the central Amazon that were correlated to *in situ* observed declines of stem diameter growth (van Emmerik et al., 2017). There is currently a lack of integrated understanding of how observed remote sensing responses to drought translate into actual responses of aboveground forest growth and functioning in tropical forests.

1.2 What is known about the drivers of stem and canopy growth?

Total plant growth or biomass production is commonly divided into leaf growth, stem and branch growth, fine and coarse root growth, as well as reproductive growth. Next to quantifying total biomass production, it is relevant to know how biomass production is partitioned, because biomass in short-lived leaves and fine roots has a much shorter residence time compared to biomass in stems, branches and coarse roots. In Neotropical forests, the relative allocation of carbohydrates to biomass production in the canopy, stem and roots varies both spatially with climate and differences in soil properties (Hofhansl et al., 2015, 2020) as well as over time with changes in water availability, air temperature and insolation (Doughty et al., 2014, 2015a; Girardin et al., 2016). Stem growth is mostly estimated using a combination of dendrometer measurements and allometric equations (e.g. Malhi *et al.*, 2009b). Canopy growth is often determined by quantifying the amount of litterfall that is collected in so-called litter traps (e.g. Chave *et al.*, 2010). In Neotropical forest plots, stem growth increases with soil phosphorus availability, soil clay fraction and mean annual precipitation (Aragão et al., 2009; Banin et al., 2014; Hofhansl et al., 2015; Quesada et al., 2009; Soong et al., 2020). In contrast, the spatial variability in canopy production between sites is not explained by differences in mean annual precipitation or soil properties (Chave et al., 2009). Therefore, the drivers of the spatial variability in canopy growth across Neotropical forests remain largely unknown.

In humid Neotropical forests, leaf flushing in the early dry season results in the increase of canopy growth and a simultaneous decline in stem growth (Doughty et al., 2014; Girardin et al., 2016; Hofhansl et al., 2014). The decline of stem growth during the dry season in humid forests is not related to a decline in overall biomass production but is related to a shift in carbohydrate allocation from the root and stem towards the canopy (Doughty et al., 2015b). In tropical dry forests, leaf litterfall increases in the dry season and leaf flushing is delayed until the start of the wet season when soil water is replenished (Sanchez et al., 2008; Selva et al., 2007). Furthermore, the rate of dry season litterfall is observed to be higher near to the forest edge compared to



the interior, associated with dryer and warmer microclimatic conditions near the forest edge (Schessl et al., 2008; Sizer et al.,
100 2000). On more wind exposed sites in the neotropics, not seasonality but the sporadic occurrence of tropical storms is driving
the temporal variability in litterfall and canopy growth (Heineman et al., 2015; Liu et al., 2018a; Veneklaas, 1991). Finally,
hot and dry conditions associated with El Niño Southern Oscillation (ENSO) and tropical North Atlantic sea surface
temperature anomalies (Marengo et al., 2011) have been linked to periods of elevated litterfall (Detto et al., 2018; Thomas,
1999) and reduced stem growth in Neotropical forests (Feldpausch et al., 2016; Phillips et al., 2009; Rifai et al., 2018;
105 Vasconcelos et al., 2012). However, it is still uncertain whether drought-induced changes in biomass production that were
observed in inventory plots, occurred on a larger regional scale in Neotropical forests.

The aims of this study are to examine, based on a novel dataset of stem growth and leaf litterfall across Neotropical ecosystems,
(1) how leaf litterfall, leaf flushing and stem growth change in response to drought, (2) reconcile *in situ* measurements of leaf
110 litterfall, leaf flushing and stem growth with remote sensing analysis, and (3) use an empirical model to estimate the impact of
historical droughts and long-term climate trends on aboveground biomass production.

2. Methods

2.1 Inventory data

We searched the available literature for reported stem growth and litterfall data collected between 1981 and 2019 at sites across
115 tropical and sub-tropical South and Central America between 30° south and 30 ° north. The search timespan was chosen to
match that of the *ERA5-Land* climate dataset that provided the explanatory variables in the empirical models (see section 2.4).
Search terms included: leaf litterfall, litterfall, litterfall production, stem growth, diameter growth, tree growth. Also the
Spanish and Portuguese literature was searched for studies that reported litterfall production with the key words: producción
de hojarasca and produção de serapilheira, respectively.

120

Monthly values of stem growth and litterfall were extracted from existing datasets as well as published manuscripts and
compiled into a new dataset together with the month and year of observation, site name, location and data source (see
Supplementary dataset). The majority of monthly data was extracted from published figures in individual manuscripts using a
freely available digitizing tool (Rohatgi, 2018). When the measurement time spanned multiple months or years, for example
125 tree census data (e.g. Brienen *et al.*, 2015), instead of a well-defined year and month of observation, we included the start and
end date of the census interval in the dataset. Total fine litterfall (including leaves, fruits, flowers and twigs) and leaf litterfall
were, whenever possible, separately retrieved from the literature. When only leaf litterfall or total fine litterfall was provided
in the original study, which was the case for 123 out of 211 studies that reported litterfall data, the missing litterfall data was
estimated from a linear relationship between leaf litterfall and total fine litterfall ($R^2= 0.93$, $p < 0.01$, $n = 3034$, Figure S1). All
130 litterfall and stem growth data was converted to $\text{Mg C ha}^{-1} \text{ month}^{-1}$ using 50% carbon content per unit of biomass. The database



counted 7228 individual observations of litterfall and 2732 observations of stem growth that were retrieved from 246 studies conducted at 814 sites in the neotropics.

Litterfall observations can be used to estimate canopy growth at a specific site on multi-year timescales. However, monthly
135 litterfall cannot be directly used to estimate monthly canopy growth as shed leaves are not instantly replaced by the same amount of newly flushed leaves. Therefore, we estimated monthly leaf flushing or leaf growth following Doughty & Goulden (2009) as:

$$Leaf\ flush = \frac{\Delta LAI}{SLA} + Leaf\ litterfall \quad (1)$$

140

where *Leaf litterfall* is the measured leaf litterfall ($Mg\ C\ ha^{-1}\ month^{-1}$), *SLA* is the specific leaf area ($m^2\ Mg^{-1}\ C$) and ΔLAI the monthly change in leaf area index ($m^2\ ha^{-1}\ month^{-1}$). Specific leaf area data was extracted from the global gridded plant traits product of Butler et al. (2017). Monthly LAI was extracted for each site from July 1981 until December 2018 from the
145 Global Data Set of Vegetation Leaf Area Index (LAI3g) (Zhu et al., 2013). The LAI3g is a validated global product developed using multi-spectral remote sensing data in a neural network algorithm, showing reasonable accuracy ($RMSE = 0.68\ m^2\ m^{-2}$) at ground truthing sites in various biomes and no saturation of LAI in dense broadleaf tropical forests (Zhu et al., 2013).

In addition to leaf flushing, we estimated the proportion of mature leaf area as:

$$LAI_{mature} = \sum_{n=-5}^{-2} (Leaf\ flush * SLA)_n \quad (2)$$

150

In Neotropical humid forests, newly flushed leaves take approximately two months to fully mature and reach their optimal photosynthetic capacity about 2-5 months after leaf flushing (Albert et al., 2018). Therefore, the sum of leaf area flushed between 2 and 5 months in the past, here termed the mature leaf area, was thought to be a proxy of canopy photosynthetic capacity and canopy greenness.

155 2.2 Geospatial data and derived features

Properties that were not observed at the field plots included in the database (see section 2.1) were extracted from multiple gridded geospatial datasets, including soil properties, plant traits standing biomass and climate data (Table 1). We included a broad range of geospatial datasets that could possibly be used to predict the spatial and temporal variability in stem growth and leaf litterfall.

160



Climate variables were retrieved as monthly averages from January 1981 to September 2019 at a 0.1° horizontal resolution from the *ERA5-Land* reanalysis dataset (ECMWF, 2019). In addition, hourly averages of instantaneous 10-meter wind gust were retrieved from January 1979 to September 2019 at a 0.25° horizontal resolution from the *ERA5* dataset. From the hourly averages of wind gust, the maximum wind gust in each month was calculated, which is expected to be a good indicator of sporadic high litterfall following tropical cyclones (e.g. Whigham *et al.*, 1991).

Table 1 Geospatial datasets used as explanatory variables in the XGBoost models. In brackets the native horizontal resolution of the dataset if a spatially aggregated product was used.

Product name	Variables	Horizontal resolution	Temporal coverage	Data source
Plant traits	Specific leaf area (m ² kg ⁻¹) Leaf nitrogen (mg g ⁻¹) Leaf phosphorous (mg g ⁻¹)	0.5° ~56 km	-	(Butler <i>et al.</i> , 2017)
ESA Aboveground biomass	CCI Aboveground biomass (Mg ha ⁻¹)	500 m (100 m)	2017	ESA Climate Change Initiative (Santoro and Cartus, 2019)
ALOS elevation and terrain	Elevation (m above sea level) Slope (°) Aspect (°)	1 km (90 m)	2006-2011	(Tadono <i>et al.</i> , 2014)
SoilGrids - global gridded soil data	Available soil water capacity (%) Cation exchange capacity (cmol kg ⁻¹) Bedrock depth (cm) Clay, sand and silt fractions (%) pH measured in water (index) Organic carbon content (g kg ⁻¹) Total nitrogen (g kg ⁻¹)	1 km (250 m)	-	(Hengl <i>et al.</i> , 2015, 2017)
GFPLAIN250m	Floodplain presence	250 m	-	(Nardi <i>et al.</i> , 2019)
ERA5 hourly averaged data from 1979 to present	Instantaneous 10 meter wind gust (m s ⁻¹)	0.25° ~28 km	01-01-1979 01-09-2019	(Copernicus Climate Change Service, 2019)
ERA5-Land monthly averaged data from 1981 to present	10 meter windspeed (m s ⁻¹)* Dewpoint temperature at 2m (K) Temperature at 2m (K) Evaporation (m of water equivalent) Leaf area index high vegetation (m ² m ⁻²) Surface latent heat flux (J m ⁻²) Surface net solar radiation (J m ⁻²) Surface sensible heat flux (J m ⁻²) Total precipitation (m) Volumetric soil water in four layers (m ³ m ⁻³) Skin reservoir content (m)	0.1° ~11 km	01-01-1981 01-09-2019	(Copernicus Climate Change Service, 2019)



The number of explanatory variables, from here on called features, was further expanded by calculating derived features from the aforementioned datasets. Providing the empirical model with a large variety of often related features helps building performant models with a relatively low number of dependent variables (Guyon and Elisseeff, 2003). The soil C:N ratio was calculated by dividing soil organic carbon content (g kg^{-1}) by soil total nitrogen content (g kg^{-1}) from the SoilGrids dataset (Hengl et al., 2017). Furthermore, the leaf N:P ratio was calculated from the leaf nitrogen (mg g^{-1}) and leaf phosphorus content (mg g^{-1}) present in the global gridded plant trait dataset (Butler et al., 2017). The gridded leaf N:P ratio was included into the empirical model as the gradient in plant available phosphorus is a key driver of forest structure and productivity across the Amazon basin (Quesada et al., 2012). Finally, the distance to the forest edge was calculated from the 500-meter horizontal resolution aboveground biomass map as the Euclidean distance between every cell and the nearest cell with an aboveground biomass value below an arbitrary threshold of $50 \text{ Mg biomass ha}^{-1}$ (considered not forest). Because of the relatively high horizontal resolution (500 m) of the aboveground biomass map, the distance to the forest edge could not only identify the distance to large clearings and transitions to more open biomes but also the distance to smaller clearings and rivers.

To further expand the number of features available to train the model and to include historical climate data to the model, all monthly climate data up to 1 year in the past were separately added to the model. In this way, the model cannot only choose to use, for example, total precipitation in the present month but also the total precipitation in the previous month and the total presentation in the same month one year in the past to model stem growth and leaf litterfall in that particular month.

2.3 Remote sensing data

Reconciling differences between remote sensing observations from different sensors, as well as reconciling field and remote sensing observations required long-term records of remote sensing products from different sensors. The enhanced vegetation index (EVI) from the moderate resolution imaging spectroradiometer (MODIS) vegetation index product (MOD13C2 version 6) was used as an indicator of vegetation greenness (Gao et al., 2000). EVI is regarded as an improved vegetation index compared to the normalized difference vegetation index (NDVI), as it relies on the blue band next to the red and near infrared bands and uses aerosol resistance coefficients in its formulation (Huete et al., 2000). The data were acquired from the website of the United States Geological Survey on a 0.05° grid with a 16 day temporal resolution from February 2000 up to April 2020 (Didan, 2015). The images were averaged to monthly values to be able to compare the EVI to the empirically modelled stem growth, leaf litterfall and leaf flushing data.

In addition, we used remotely sensed sun-induced fluorescence (SIF) data as a proxy of canopy photosynthesis. The SIF data used was retrieved from the recent Sun-Induced Fluorescence of Terrestrial Ecosystems Retrieval version 2 dataset (SIFTER v2). The SIF measurements are derived from hyperspectral observations of the GOME-2 sensor onboard the Metop-A satellite (Schaik et al., 2020). Point observations of SIF were projected on a 0.5° global grid and spatially aggregated to monthly averages for comparison with the field data and other remote sensing datasets.



205 Finally, monthly data was also available for vegetation optical depth (VOD), a passive microwave product (Liu et al., 2013; Meesters et al., 2005). VOD is directly proportional to the vegetation water content, and therefore sensitive to canopy density and biomass (Jackson and Schmugge, 1991; Meesters et al., 2005; Owe et al., 2001). Furthermore, the advantage of VOD compared to the MODIS EVI is that VOD is unaffected by cloud cover. VOD has been used recently to study vegetation phenology (Jones et al., 2011, 2014) and to monitor global vegetation dynamics (Andela et al., 2013; Liu et al., 2007, 2013, 210 2015) and deforestation (van Marle et al., 2016). We used C band and X band VOD data from the global long-term Vegetation Optical Depth Climate Archive (Moesinger et al., 2020).

2.4 Data analysis

Machine learning enables integrating the different spatial and temporal scales inherent to the field observations in a single method and making predictions based on the trends identified in the data. Extreme gradient boosting (XGBoost), a machine 215 learning method for classification and regression (Chen and Guestrin, 2016) was used to upscale *in situ* measurements to estimate monthly leaf litterfall and stem growth rates for the neotropics from 1982 to 2019.

The XGBoost algorithm was selected for its demonstrated performance when applied to similar environmental science problems such as soil mapping (Hengl et al., 2017) and estimating evapotranspiration (Fan et al., 2018). Like other boosting 220 algorithms, XGBoost uses an ensemble of weak prediction models, iteratively building each new model to improve the prediction of the ensemble of previous models. In essence, XGBoost constructs a series of relatively shallow regression trees that provide a continuous output value at each leaf, these output values are summed over all regression trees to derive the final prediction. The output value of each regression tree is scaled by a predetermined factor η (learning rate) which reduces the weight of the individual tree. Adjusting this factor vigilantly ensures a smooth descent of the loss function (Chen and Guestrin, 225 2016). Besides the learning rate, XGBoost enables the use of multiple other regularization options. The parameters modulating the regularization options in the model (so-called hyperparameters) are tuned to make the final model more robust and prevent overfitting on the training data. Here, we use the R package *xgboost* (Chen et al., 2020) to construct the model and the R package *mlr* (Bischl et al., 2020) to tune hyperparameters and select the final features used in the model.

230 Two XGBoost models were constructed, to estimate leaf litterfall and stem growth separately. Before setting up the models, the stochastic behaviour present in the monthly timeseries of leaf litterfall and stem growth was reduced by using a moving average filter with a window size of 3 months. Furthermore, positive outliers, defined as values higher than 3 times the standard deviation above the mean, were omitted. The monthly climate data linked to the stem growth and leaf litterfall observations spanning multiple months to years was averaged using the start date and end date of the observation interval. To account for 235 the difference in observation timespan, weights were assigned to the observations in the model as following:



$$\text{Observationweight} = 1 + \ln(n_{\text{months}}) \quad (3)$$

where n_{months} is the length of the time interval in months. By using the natural logarithm to assign weights, observations covering multiple months to years were assigned 2 to 5 times the weight of a monthly observation. This was preferred in contrast to assigning weights directly proportional to the length of the time interval as this would inflate the importance of a few sites with very long observation time intervals in the model.

Model performance was evaluated by dividing all leaf litterfall and stem growth data into a training dataset containing 60% of all observations at each site and a test dataset containing the remaining 40% of the observations. The initial XGBoost model was constructed using the default learning rate (0.3) and the best model iteration was estimated using a 10-fold cross-validation of the training data, selecting the iteration with the lowest root mean squared error (RMSE) on the cross-validated data. Next, we filtered out 80% of the initial 235 features with the lowest feature importance (gain) to reduce the dimensionality of the data and speedup subsequent tuning. Hyperparameter tuning of all the model parameters was done by random search using 1000 iterations and 10 fold cross-validation. Subsequently, feature selection was done to select a maximum of 20 features for each model with the updated hyperparameters and random search using 1000 iterations and 10 fold cross-validation.

To evaluate the drought responses of modelled stem growth, leaf litterfall and leaf flushing, two rectangular drought areas were delineated within the Amazon basin for the 2005 and the 2015 drought period. First, the drought period was identified for both droughts using the average ERA5 topsoil moisture content for the entire Amazon basin. For each month in the time series, the seasonally detrended topsoil moisture content was calculated by subtracting the monthly average and dividing by the standard deviation of that month. The drought period was defined as the consecutive months with a topsoil moisture content below one standard deviation (σ) compared to its monthly average. Subsequently, a rectangular area was delineated that overlapped those areas within the Amazon basin that showed a topsoil moisture content $< 1.5 \sigma$ averaged over the entire drought period.

3. Results

3.1 Model evaluation and feature importance

The two XGBoost models, one for stem growth (NRSME = 11.2%) and one for leaf litterfall (NRMSE = 9.5%), showed a comparable accuracy across the 40% of the data that were used to evaluate the models (Figure 1a, 1c). The model predicting stem growth showed less uncertainty in absolute metrics (RMSE = 0.06 Mg C ha⁻¹ month⁻¹) compared to the model predicting leaf litterfall (RMSE = 0.08 Mg C ha⁻¹ month⁻¹). However, the range in observed values and the explained variation was smaller for the stem growth model ($R^2 = 0.51$) compared to the leaf litterfall model ($R^2 = 0.67$). In both models, high rates of stem growth and leaf litterfall were consistently underestimated while relatively low values were overestimated (Figure 1a, 1c).



270 Of the 235 features that were used in the first XGBoost models, only 20 features were used in the two final models. These
features have been ranked based on their importance (gain) in these final models and the top tens of most important features
in both models are shown (Figure 1b, 1d). The most important features explaining the spatial and temporal variability in stem
growth and leaf litterfall that were used in both models included the distance to the forest edge, terrain elevation, soil moisture
content, vapour pressure deficit, soil pH, leaf nitrogen content and specific leaf area. Additional features explaining stem
275 growth included precipitation and runoff, terrain aspect, bedrock depth, air temperature and evaporation, and leaf N:P ratio
(Figure 1b). The spatial and temporal variability in leaf litterfall was further explained by features including aboveground
biomass, meteorological variables such as dewpoint temperature and net solar radiation and soil properties such as cation
exchange capacity, C:N ratio, soil nitrogen content and soil sand fraction (Figure 1d). Although the importance of some of
these features in the models might represent a causal link with either stem growth or leaf litterfall, we cannot conclude from
280 this empirical analysis that this is the case.

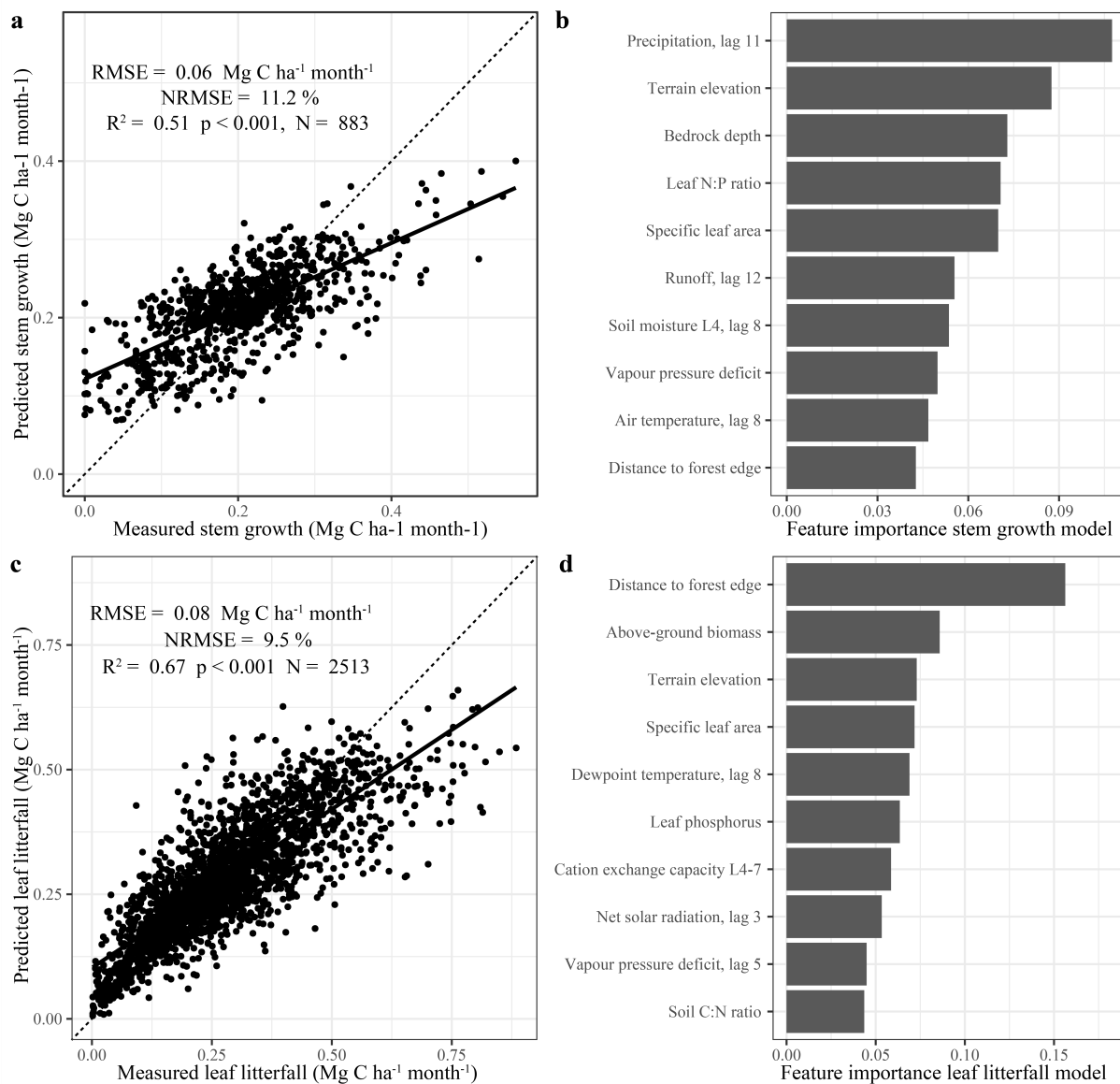


Figure 1 Model evaluation and feature importance. The scatterplots on the left side of the figure (a, c) show the predicted biomass production versus the measured biomass production of the test data that was used to validate the stem growth (a) and leaf litterfall (b) models. The dashed black line is the 1:1 line and the solid black line the least squares linear regression fit. The bar graphs on the right side of the figure (b, d) show the feature importance (gain) of the top 10 features selected for the final models. Feature names are detailed in Table 1. Features with lags indicate the value of that climate variable a given number of months in the past (e.g. precipitation lag 11 is the monthly precipitation 11 months in the past).

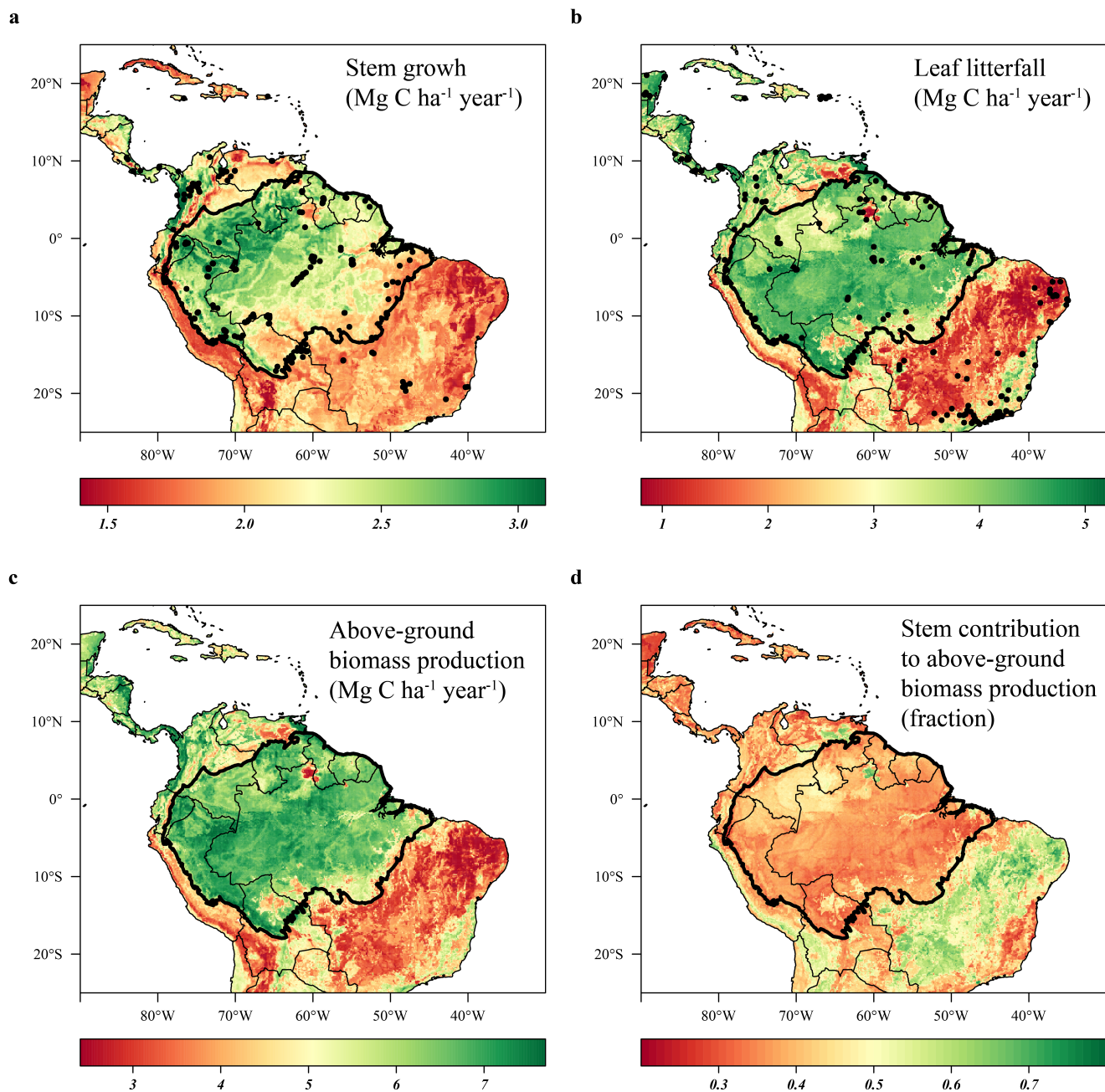
285



3.2 Long-term stem growth and leaf litterfall rates across the neotropics

290 Distinct spatial patterns in stem growth and leaf litterfall rates across the neotropics arose in the long-term (1982-2019)
predicted data (Figure 2). The range of predicted leaf litterfall rates ($0.8 \sim 5.0 \text{ Mg C ha}^{-1} \text{ year}^{-1}$) across the Neotropics was
more than two times as large as the range of predicted stem growth ($1.4 \sim 3.1 \text{ Mg C ha}^{-1} \text{ year}^{-1}$), in accordance with the observed
difference in the range of the field data (Figure 1a, 1b). Although the spatial patterns in stem growth and litterfall rates differed,
some general trends can be identified. Relatively low rates of predicted stem growth and leaf litterfall are observed in the
295 savanna and xeric shrub ecosystems of the Neotropics such as the Cerrado and Caatinga in Brazil, the Llanos savanna in
Venezuela and the Beni savanna in Bolivia (Figure 2a, 2b). Furthermore, low stem growth and leaf litterfall rates are also
observed in the montane environments of the Andes (Figure 2a, 2b). Relatively high rates of predicted stem growth are found
in Central America, along the Pacific coast of Colombia and in the northern and western Amazon basin (Figure 2a). Leaf
litterfall showed relatively high rates in the Atlantic forests of south-eastern Brazil, in Central America and across the forest
300 covered Amazon basin (Figure 2b).

As the range in predicted leaf litterfall rates was much larger than the range in predicted stem growth rates, the spatial variability
in leaf litterfall rates largely drives the spatial variability in aboveground biomass production across the Neotropical ecosystems
(Figure 2c). Furthermore, the predicted stem growth and leaf litterfall data shows that in areas with a relatively low
305 aboveground biomass production, for example in the Cerrado region and the Andes, the contribution of stem growth to the
total aboveground biomass production is relatively large (> 0.45). In contrast, in areas where aboveground biomass production
is relatively high, for example in the Amazon basin and Central America, the contribution of stem growth to the total
aboveground growth is relatively low (< 0.45 , Figure 2d). Also noteworthy is that the always wet north-western Amazon basin,
that experiences no seasonality in precipitation (Sombroek, 2001), shows relatively high stem growth and low leaf litterfall
310 rates compared to the other regions within the basin (Figure 2a, 2b). These results suggest that as productivity increases in
these Neotropical ecosystems, an increasingly larger proportion of available carbohydrates is allocated to the production of
leaves.



315 **Figure 2** Predicted stem growth, leaf litterfall and total aboveground biomass production and the contribution of stem growth to the aboveground biomass production across the neotropics from 1982 to 2019. Site locations where stem growth (n = 458) (a) and leaf litterfall (n = 377) (b) were measured are depicted as solid black circles. Country borders and the extent of the Amazon basin are marked by thin and thick black lines, respectively.

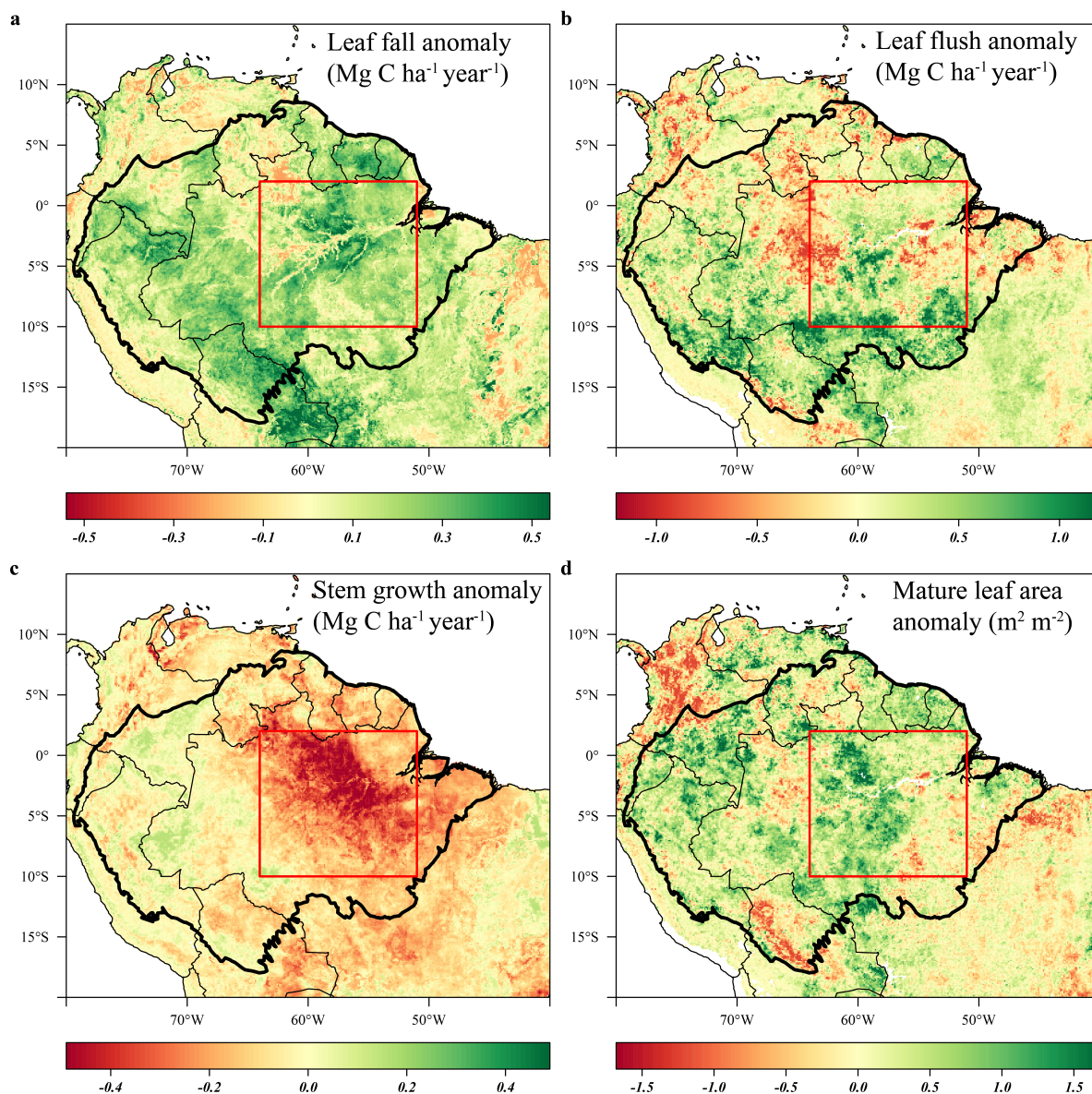


3.3 Aboveground growth responses to the drought of 2015

The predicted monthly stem growth and leaf litterfall data were used to estimate the impact of the 2015 drought in the Amazon region. Across the entire Amazon basin, leaf fall generally showed positive anomalies while stem growth showed negative anomalies during the 2015 drought (August 2015 to January 2016, Figure 3a & 3c). However, significant regional differences in the responses of leaf fall, leaf flushing and stem growth to the 2015 drought were observed within the Amazon basin (Figure 3). A combination of positive seasonal anomalies in leaf fall and leaf flushing and negative anomalies in stem growth during the 2015 drought were mainly observed in the eastern Amazon that was delineated as the drought area (red rectangle in Figure 3 and 4). This area experienced the most significant negative anomalies in top-soil volumetric moisture content and positive anomalies in net solar radiation (Figure 4a & 4b). During the height of the drought in November 2015, precipitation (-1.7σ) and soil moisture (-2.6σ) were significantly lower in the drought area compared to their monthly average, while air temperature ($+2.7 \sigma$, not shown), vapor pressure deficit ($+2.8 \sigma$) and solar radiation ($+2.1 \sigma$) were all significantly higher compared to their monthly average (Figure 5c). In the western Amazon, that experienced less severe drought conditions in 2015 (Figure 4), leaf fall and leaf flushing were also enhanced while stem growth showed no apparent negative nor positive anomalies (Figure 3).

From August 2015 to January 2016 stem growth was on average significantly lower (-1.8σ) in the drought area while leaf fall was higher ($+0.9 \sigma$) compared to the long-term averages of stem growth and leaf fall for these months (Figure 5a). Predicted stem growth remained lower in the drought area after the end of the drought in the remaining 11 months of 2016 (-1.5σ , Figure 5a). Furthermore, leaf flushing was higher than the monthly average at the onset ($+1.9 \sigma$ in August 2015) and end of the drought ($+0.8 \sigma$ in January 2016) following the first rain events (not shown). During the height of the drought (-1.3σ in November 2015, Figure 5) leaf flushing was lower than the monthly average.

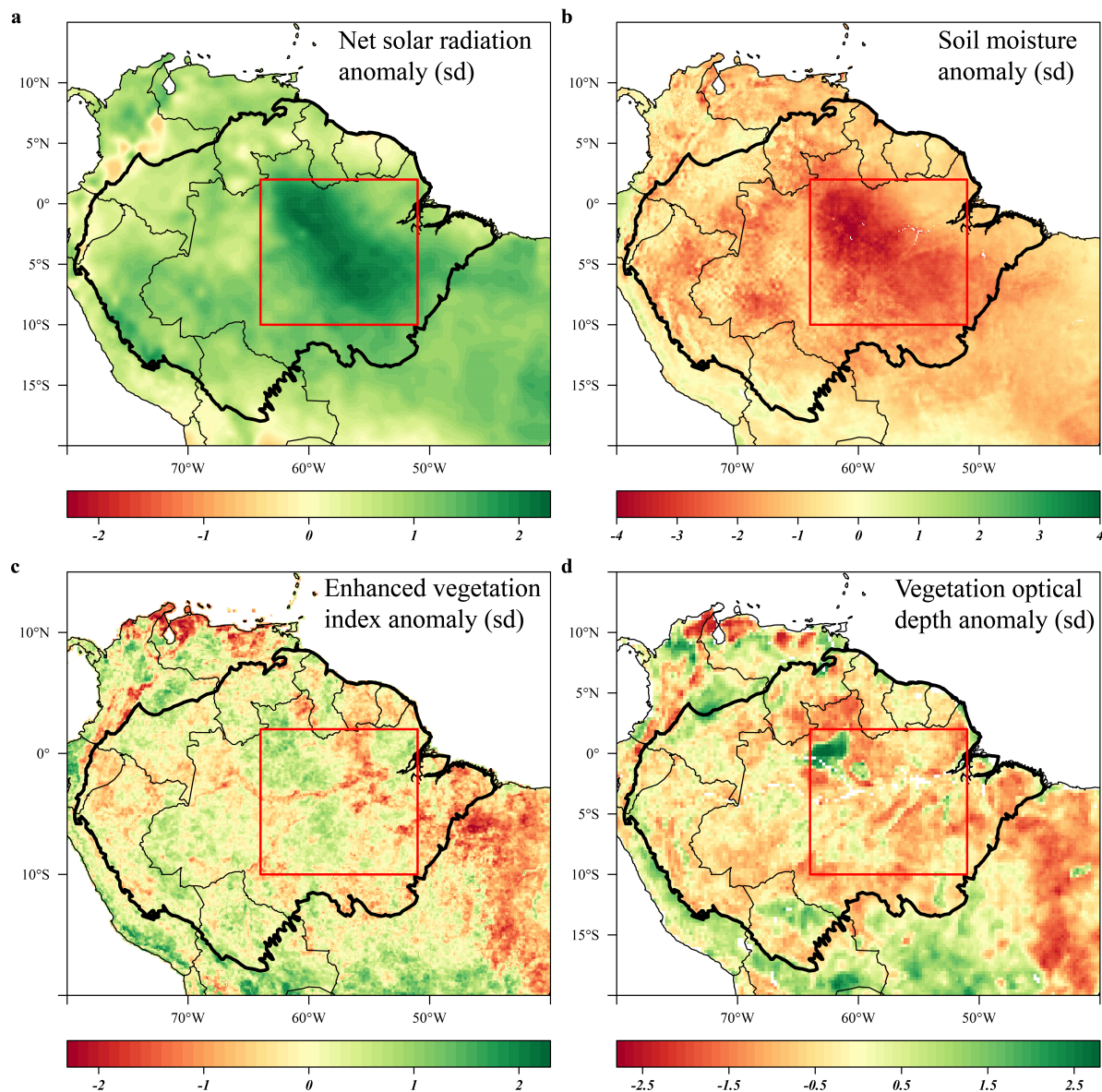
In the drought area, anomalously high leaf flushing at the onset of the 2015 drought resulted in an above average mature leaf area (i.e. the sum of leaf area flushed in the past 2-5 months), in the second half of the drought ($+1.3 \sigma$ in October 2015 - January 2016, Figure 5a). The spatial pattern of the positive anomalies in mature leaf area coincided with positive anomalies in EVI (Figure 3d & 4c). Green-up during drought was visible as positive anomalies in predicted mature leaf area and EVI in eastern Colombia and in the central Brazilian Amazon (Figure 3d & 4c). In contrast, the X band vegetation optical depth (VOD) and sun-induced fluorescence (SIF) showed widespread negative anomalies in the drought area (-0.8σ and -2.4σ in September - November, respectively) during the height of the 2015 drought (Figure 4c & 5b). Note the contrast in the observed responses between the moist tropical forest of the Amazon basin with the Cerrado and Caatinga regions of eastern Brazil. In the dryer Cerrado and Caatinga regions, leaf flushing, mature leaf area, VOD and EVI all show clear negative anomalies during the 2015 drought (Figure 3 & 4).



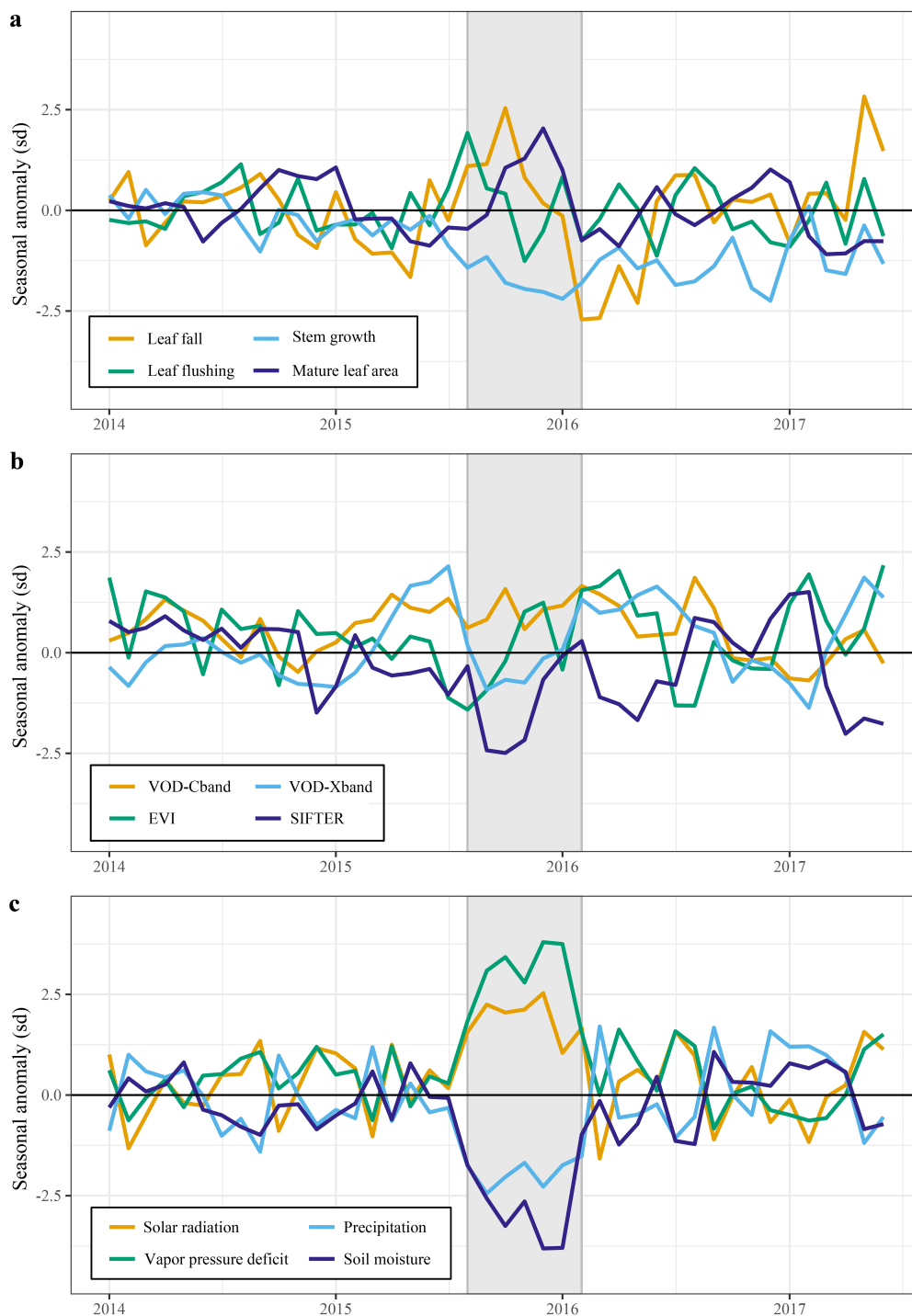
350

355

Figure 3 Average anomalies in leaf fall, leaf flushing, stem growth and mature leaf area during the 2015 drought (August 2015 – January 2016) compared to their long-term averages (1982–2019). Leaf fall (a) and stem growth (c) were directly retrieved from the long-term monthly model estimates. Leaf flush (b) was calculated from monthly predicted leaf fall (a) and changes in LAI (Eq. 1). Mature leaf area (d) is the sum of new leaf area flushed in the previous 2 to 5 months (Eq. 2). Country borders and the extent of the Amazon basin are marked by thin and thick black lines, respectively. The red rectangle delineates the drought area for which further results are reported.



360 **Figure 4** Standardized anomalies in net solar radiation (a), soil moisture (b), enhanced vegetation index (c) and X band vegetation optical depth (d) during the 2015 drought (August 2015 – January 2016) compared to their long-term monthly averages. Soil moisture anomalies are calculated from the ERA-5 volumetric soil moisture in the first soil layer (L1). Country borders and the extent of the Amazon basin are marked by thin and thick black lines, respectively. The red rectangle delineates the drought area for which further results are reported.



365 **Figure 5** responses of aboveground growth and remotely sensed vegetation properties to the 2015 ENSO drought and key climatic variables. All graphs show the trend in the standardized seasonal anomaly, the deviation from the monthly mean divided by the standard deviation of that month. Leaf fall and stem growth (a) are derived from the two separate XGBoost models providing monthly values from January 1982 until September 2019. Mature leaf area (a) is the sum of flushed leaves from 2 to 5 months in the past



370

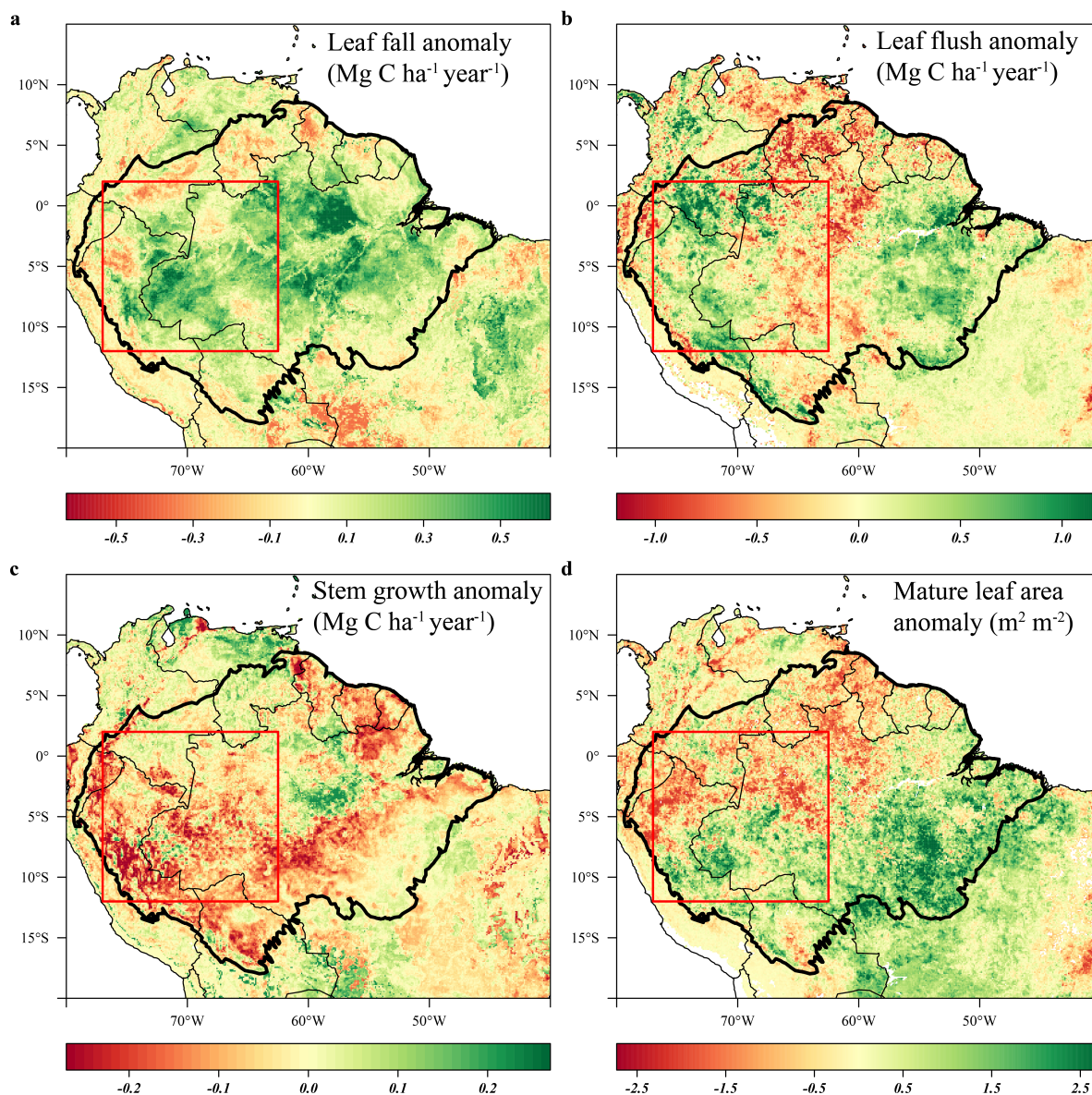
3.4 Aboveground growth responses to the drought of 2005

The long-term records of predicted leaf litterfall, leaf flushing and stem growth enable looking back at changes in estimated growth that occurred in response to other historic droughts. The drought of 2005 has been considered a particularly severe drought in the western Amazon and was the first major drought captured by the MODIS sensors which led to the first
375 observations of Amazon forest green-up during drought (Saleska et al., 2007).

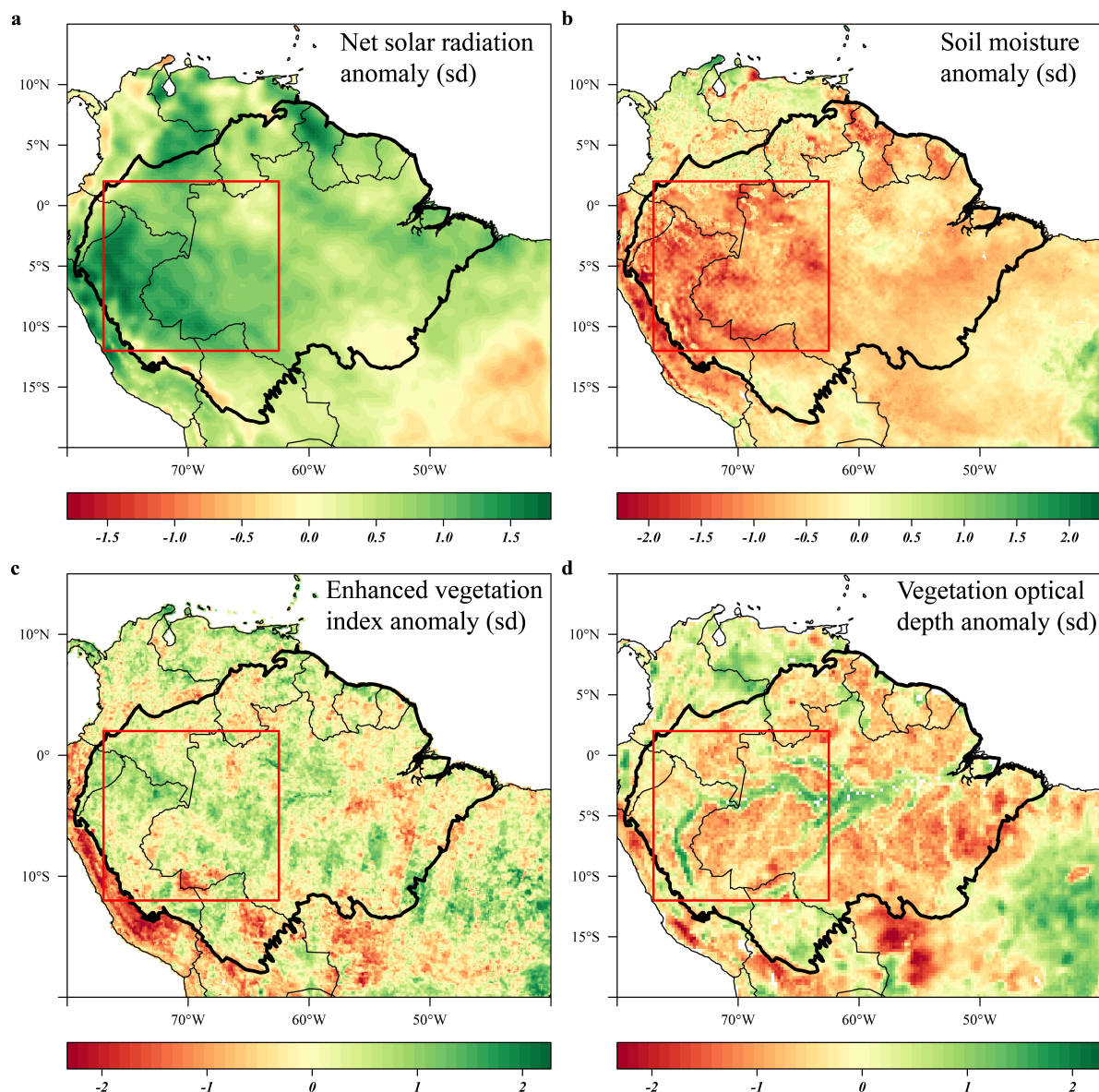
Similar to the 2015 drought, we find that leaf flushing was significantly higher at the onset (+1.1 σ in June 2005) and at the end of the drought (+0.7 σ in September – October 2005) and lower at the height of the drought (-1.3 σ in July 2005) compared to the long-term monthly average (Figure 8a). The enhanced leaf flushing at the end of the 2005 drought also marked the end
380 of the 2005 dry season with the first rain events occurring in August (not shown). Enhanced leaf flushing at the onset of the 2005 drought resulted in a higher mature leaf area (+1.1 σ in August 2005) at the end of the drought (Figure 6b & 8a). Also similar to 2015, leaf fall was elevated while stem growth was lower during the 2015 drought (+0.9 σ and -0.6, respectively, in June to September 2005). Stem growth remained lower a full year after the drought (Figure 5a).

385 The new generation of algorithms and the longer time-series of MODIS EVI data confirm the findings of Saleska *et al.* (2007), i.e., that EVI was significantly and consistently higher during the 2005 drought, compared to the long-term average (Figure 7c). EVI was significantly elevated before and at the onset of the 2005 drought (+1.94 σ) in March to May 2005 and remained higher during the height of the 2005 drought (+1.3 σ) in June to August 2005 (Figure 8b). Similar to 2015, we find that X band VOD was significantly lower in the drought area during the height of the 2005 drought (-1.2 σ) in June to August 2005 while
390 C band VOD did not show a clear effect of the 2005 drought (Figure 8b).

During the 2005 drought (June-September), precipitation (-1.5 σ) and soil moisture (-1.3 σ) were lower compared to their monthly averages in the drought area (Figure 7b & 8c). Air temperature (+0.9 σ), vapour pressure deficit (+1.4 σ) and solar radiation (+1.3 σ) were all higher during the 2005 drought compared to their monthly averages (Figure 7a & 8c). The duration
395 of the 2005 drought (~4 months) was shorter compared to the 2015-2016 drought (~6 months) and when comparing the seasonal anomalies of the climatic variables in the drought areas, the 2015 drought was clearly more severe and more anomalous compared to the 2005 drought (Figure 5c & 8c).



400 **Figure 6** Average anomalies in leaf fall, leaf flushing and stem growth and mature leaf area during the 2005 drought (June – September 2005) compared to their long-term monthly averages (1982-2019). Leaf fall (a) and stem growth (c) were directly retrieved from the long-term monthly model estimates. Leaf flush (b) was calculated from monthly predicted leaf fall (a) and changes in LAI. Mature leaf area (d) is the sum of new leaf area flushed in the previous 2 to 5 months. Country borders and the extent of the Amazon basin are marked by thin and thick black lines, respectively. The red rectangle delineates the drought area for which further results are reported.



405

Figure 7 Seasonal anomalies in net solar radiation (a), soil moisture (b), enhanced vegetation index (c) and X band vegetation optical depth (d) during the 2005 drought (June – September 2005) compared to their long-term monthly averages (1982-2019). Soil moisture anomalies are calculated from the ERA-5 volumetric soil moisture in the first soil layer (L1). Country borders and the extent of the Amazon basin are marked by thin and thick black lines, respectively. The red rectangle delineates the drought area for which further results are reported.

410

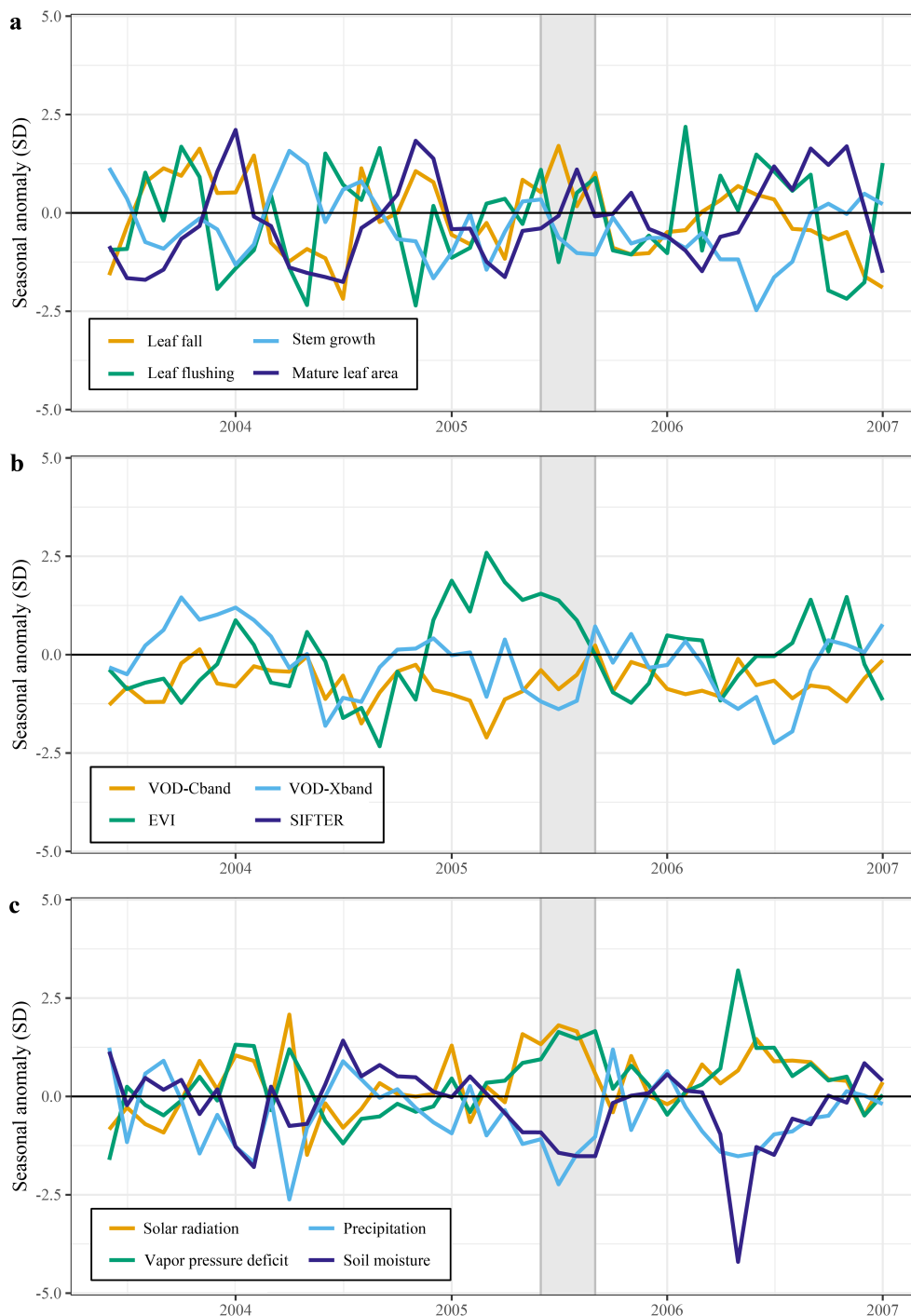


Figure 8 responses of aboveground growth and remotely sensed vegetation properties to the 2005 drought (June – September 2005) and key climatic variables. All graphs show the trend in the standardized seasonal anomaly, the deviation from the monthly mean divided by the standard deviation of that month. Leaf fall and stem growth (a) are derived from the two separate XGBoost models providing monthly values from January 1982 until September 2019. Mature leaf area (a) is the sum of flushed leaves from 2 to 5 months in the past.

415

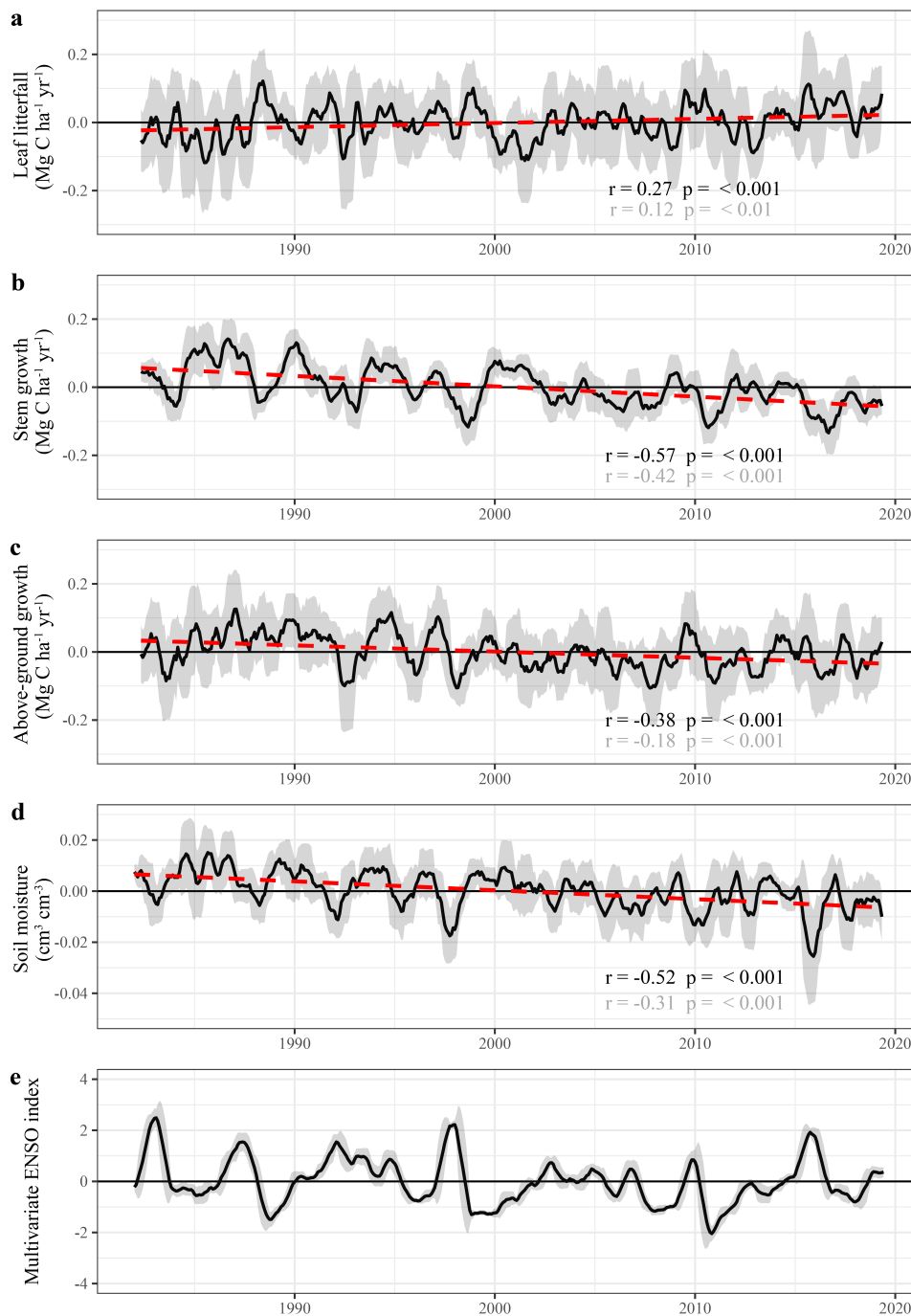


3.5 Long-term trends and ENSO effects on aboveground growth

The predicted long-term monthly stem growth and leaf litterfall values were seasonally detrended (i.e. subtracting the monthly average to omit seasonality) to identify long-term trends and multi-year fluctuations in aboveground biomass production (Figure 9). The following statistics are derived from the timeseries that have been seasonally detrended and which have been smoothed using a moving average (Figure 9, black line). The seasonally detrended data suggests a significant decline ($r = -0.38$, $p < 0.001$, $-1.84 \cdot 10^{-3} \pm 0.5 \cdot 10^{-3} \text{ Mg C ha}^{-1} \text{ yr}^{-2}$) of aboveground biomass production in the Amazon basin since 1982 (Figure 9c). This change in biomass production is driven by a decline in stem growth ($r = -0.57$, $p < 0.001$, $-3.04 \cdot 10^{-3} \pm 0.21 \cdot 10^{-3} \text{ Mg C ha}^{-1} \text{ yr}^{-2}$) which offsets the observed increase of leaf production ($r = 0.27$, $p < 0.001$, $1.22 \cdot 10^{-3} \pm 0.21 \cdot 10^{-3} \text{ Mg C ha}^{-1} \text{ yr}^{-2}$) between 1982 and 2019 (Figure 9a & 9b).

The significant decline of stem growth and increase of leaf litterfall over time in the Amazon basin is possibly driven by the warming and drying of the Amazonian climate. While surface air temperature was found to have increased between 1982 and 2019 ($r = 0.58$, $p < 0.001$, $1.97 \cdot 10^{-2} \pm 0.13 \cdot 10^{-2} \text{ °C yr}^{-1}$) top-soil volumetric moisture content declined ($r = -0.52$, $p < 0.001$, $-3.35 \cdot 10^{-4} \pm 0.26 \cdot 10^{-4} \text{ m}^3 \text{ m}^{-3} \text{ yr}^{-1}$, Figure 9d). However, distinct regional differences are visible in the trends of leaf litterfall, stem growth, top-soil volumetric moisture content and vapour pressure deficit (Figure S2). While the central Brazilian Amazon shows a significant ($p < 0.05$) drying trend coinciding with a clear negative trend in stem growth, large areas within Suriname, Guyana and eastern Venezuela show regional wetting and also a significant increasing trend of stem growth and leaf litterfall.

Superimposed on the long-term trends is the short-term variability in leaf litterfall, stem growth and aboveground biomass production that seem strongly related to El Niño oscillations (Figure 9d). This is to be expected as the climate variables used to estimate leaf litterfall and stem growth are also strongly impacted by ENSO. However, it is still noteworthy that three major ENSO related droughts in 1997, 2010 and 2015 can be identified as periods with relatively low soil moisture, high leaf litterfall, low stem growth and low total aboveground biomass production (Figure 9).



440

445

Figure 9 Long-term predictions of seasonally detrended anomalies in aboveground growth and soil moisture across the Amazon basin and the relation with the multivariate ENSO index. Black lines are the 9 month moving average of the anomalies and the dark grey uncertainty bands show the moving standard deviation of the same data. Red dashed lines represent the least squares linear regression fit through the averaged time-series. Test statistics are provided for both the linear regression of the moving average (black) and the original monthly data (grey).



4. Discussion

4.1 Drought effects on leaf phenology and canopy productivity in Neotropical forests

450 This study aimed to investigate how leaf litterfall, leaf flushing and stem growth change in response to drought in Neotropical forest. The long-term empirically modelled estimates of leaf fall showed that during the peak of the 2005 and 2015 droughts in the Amazon basin, leaf fall was significantly higher compared to its monthly averages in these months. Furthermore, estimated leaf fall was also elevated during other historical droughts in 1987, 1997 and 2009-2010 across the Amazon basin (Figure 9). These results confirm earlier site specific studies that reported elevated leaf litterfall during drought (Bonal et al., 2008; Rice et al., 2008; Roberts et al., 1990; Wieder and Wright, 2001) and during periods of warm and dry conditions associated with a strong El Niño event (Detto et al., 2018; Thomas, 1999). A straightforward explanation of the observed increase in leaf litterfall during drought is that leaf shedding directly reduces tree water use. Next to a progressive closure of the leaf stomata to limit transpiration, many Neotropical tree species are found to shed their leaves and thereby reduce the demand of water during drought (Wolfe et al., 2016). Therefore, leaf shedding in trees helps to limit transpiration during drought and maintain the hydraulic integrity of the water transporting tissue (Janssen et al., 2020b; Wolfe et al., 2016).

460 In contrast to leaf litterfall, the estimated seasonally detrended timeseries of leaf flushing showed positive anomalies in the early and final months of the 2005 and 2015 droughts (Figure 5a, 8a). Especially the pulse of newly flushed leaves in the early months of the 2005 and 2015 droughts resulted in above-average mature leaf area (i.e. the sum of leaf area flushed in the past 2-5 months) during the peak of both droughts. Those areas in the Amazon basin that experienced increased leaf flushing and showed a higher mature leaf area in 2005 and 2015 also showed higher values of the MODIS enhanced vegetation index (EVI). 465 These results therefore corroborate the finding that during the 2005 and 2015 droughts, large areas within the Amazon basin showed a green-up, visible as positive anomalies in the MODIS EVI (Saleska et al., 2007; Yang et al., 2018). Furthermore, these findings support *in situ* observations that showed that leaf flushing was significantly enhanced at the end of the 2015 drought in the central Amazon, resulting in higher mature leaf area, associated with positive EVI anomalies in the year 470 following the drought (Gonçalves et al., 2020).

Vegetation indices, such as the EVI and the normalized difference vegetation index (NDVI) are sensitive to vegetation chlorophyll content or “greenness” and have often been used to assess the effect of drought on the Amazon forest canopy. The earliest effects of droughts observed with satellites occurred during the 1983 and 1987 ENSO events, which caused negative anomalies in the NDVI from the NOAA Advanced Very High Resolution Radiometer (AVHRR) (Asner et al., 2000; Batista et al., 1997). However, a later ENSO related drought in 1997 resulted in positive AVHRR NDVI anomalies across the Amazon basin (Dessay et al., 2004). Furthermore, during the 2005 drought, positive anomalies in MODIS EVI were visible across the



south-western Amazon, suggesting that the forest canopy greens-up in response to drought (Liu et al., 2018b; Saleska et al., 2007). This finding has been disputed and was contributed to insufficient atmospheric correction (Asner and Alencar, 2010; 480 Samanta et al., 2010) and structural changes in the forest canopy (Anderson et al., 2010). However, our results suggest that the observed green-up during the 2005 and the later 2015 droughts might not be an artefact in the remote sensing data but an actual result of increased leaf flushing at the onset of drought.

It is noteworthy that droughts in which green-up has been observed (1997, 2005 and 2015) occurred during the second half of 485 the year (June – December), which is the dry season in the eastern Amazon (Sombroek, 2001). Contrastingly, droughts in which no green-up was observed (1983, 1987, 2010) occurred predominantly in the first half of the year and therefore in the wet season. As leaf exchange in the Amazon basin occurs in the dry season, drought conditions might accelerate leaf flushing synchronous to the general phenology in the dry season but not in the wet season. That green-up during drought occurs despite the observed positive anomalies in leaf litterfall suggests that during drought, older leaves with lower photosynthetic capacity 490 and higher NIR absorptance (Doughty and Goulden, 2009; Kitajima et al., 2002; Roberts et al., 1998) are shed, while newly flushed leaves are maintained. When taking into account the time that newly flushed leaves need to fully expand and attain their highest photosynthetic capacity, which is 2-5 months (Albert et al., 2018; Gonçalves et al., 2020; Restrepo-Coupe et al., 2013), it can be argued that the observed green-up is not a direct effect of drought but rather a consequence of the environmental conditions at the onset of the drought.

495 Earlier studies hypothesized that increased incoming solar radiation during drought, as a result of a decline in cloud cover, might be driving the observed green-up (Saleska et al., 2007). Indeed, both spatial as well as temporal correlations between photosynthetic active radiation (PAR) and EVI were found in response to the 2015 drought (Yang et al., 2018). Lengthening of the photoperiod has been recognized as a key environmental cue for leaf abscission and flushing across evergreen tropical 500 forests (Borchert et al., 2002, 2015; Elliott et al., 2006). Reduced cloud cover and increased direct solar radiation reaching the forest canopy at the onset of an atmospheric drought, when soil water is still readily available, might therefore present an environmental cue for leaf flushing. This mechanism might explain the positive anomalies in leaf flushing observed at the onset of the 2005 and 2015 droughts (Figure 5a, 8a). Next to insolation, trees need to be well hydrated to enable cell expansion, bud break and consequently leaf flushing (Borchert et al., 2002). Also the presence of older leaves in the canopy can inhibit 505 leaf flushing (Borchert et al., 2002). Therefore, the excessive shedding of older leaves during the height of the 2005 and 2015 droughts and tree rehydration following the first rain events (not shown) could have acted as a strong environmental cue for the second leaf flushing events that were observed at the end of both droughts (Figure 5a & 8a).

4.2 Drought effects on stem growth in Neotropical forests

In contrast to the observed leaf flushing and leaf fall responses to drought, stem growth is significantly reduced in the drought 510 areas of the Amazon basin during the 2015 drought and to a lesser extent in 2005 (Figure 3c & 6c). Other historical droughts



in the Amazon basin in 1987, 1997 and 2009-2010 are clearly visible in the long-term estimates as periods of reduced soil moisture and reduced stem growth across the basin (Figure 9). These results generally confirm site specific studies that found significant stem growth reductions in Neotropical forests in response to drought. These include the 1997 and 2010 droughts in Costa Rica (Clark et al., 2003; Hofhansl et al., 2014), the 2008 drought in French Guiana (Stahl et al., 2010; Wagner et al., 2013), and the 2010 and 2015 droughts across the Amazon basin (van Emmerik et al., 2017; Feldpausch et al., 2016; Rifai et al., 2018). The lack of a clear negative and long-term impact of the 2005 drought on modelled stem growth in the Amazon basin might explain why field observations failed to observed significant declines in stem growth during the 2005 drought (Phillips et al., 2009).

Stem growth reductions in response to drought can be expected as tree water status and stem growth are tightly coupled. Firstly, stem wood and bark can store substantial amounts of water, which contribute 5-30% to daily water use in Neotropical tree species (Meinzer et al., 2003; Oliva Carrasco et al., 2015). About 50% of stem wood and bark volume consists of water which can in part be withdrawn during drought (Dias and Marengo, 2016; Poorter, 2008). The loss of water from elastic tissue can result in a decline of stem growth or even a decline of stem girth (Baker et al., 2002; van Emmerik et al., 2017; Reich and Borchert, 1982; Stahl et al., 2010). These elastic changes in stem volume arising from changes in stem wood and bark water content do not represent actual changes in secondary growth. However, these elastic changes are often unintentionally present in dendrometer measurements and therefore also in our dataset. Secondly, tissue dehydration during drought can cause cell turgor loss in the vascular cambium, limiting cell division and therefore actual secondary growth (Borchert, 1994; Körner and Basel, 2013; Muller et al., 2011; Worbes, 1999). Therefore, it is reasonable to assume that water availability directly reduced stem growth during drought.

The long-term estimates of stem growth in this study point to a significant negative trend in stem growth in the Amazon basin between 1982 and 2019 (Figure 9b), which was not found in a basin-wide network of inventory plots for a similar timespan (1983-2011) (Brienen et al., 2015; Hubau et al., 2020). This is surprising as 60% of the data from these same inventory plots are used to train the stem growth model and were therefore expected to show similar long-term trends. As the plot scale data is very similar, this discrepancy has to be explained by the method of upscaling these plot scale observations. Firstly, the model provides stem growth estimates for more than 54 thousand grid cells covering the entire Amazon basin whereas the measured stem growth rates are measured at around 320 inventory plots scattered across the basin (Brienen et al., 2015). Secondly, as the model uses the ERA5 long-term reanalysis data of surface air temperature, precipitation and soil moisture to estimate stem growth, trends in the stem growth estimates are therefore reflecting the trends in the climate data (Figure 9). As stem growth in the Amazon basin generally declines in the dry season when soil moisture is low and air temperatures are high (e.g. Doughty et al., 2014; Girardin et al., 2016; Janssen et al., 2020a) a trend in soil moisture and temperature might therefore result in a predicted trend in stem growth which might not necessarily be reflecting the actual trend in stem growth. Therefore, data from



545 tree census data from permanent inventory plots (Brienen et al., 2015; Hubau et al., 2020) is essential to be able to accurately model and upscale stem growth at multi-decal timescales

4.3 What are satellite sensors actually sensing?

550 The controversy surrounding the observation of Amazon canopy green-up during drought is mainly caused by differences in sensor sensitivity and the interpretation of the retrieved signals. Generally, canopy green-up is observed in multi-spectral remote sensing data during or following major droughts in the Amazon forest (Gonçalves et al., 2020; Lee et al., 2013; Liu et al., 2018b; Saleska et al., 2007; Yang et al., 2018). Our results support this canopy green-up and attribute it to enhanced leaf flushing at the onset of a drought and subsequent leaf maturation in the following months (Figure 5a & 8a). However, canopy green-up does not necessarily have to result in, or be a consequence of, an increase in canopy photosynthesis or gross primary productivity. Indeed, *in situ* leaf scale photosynthesis is generally observed to decline during drought in Neotropical forests (Bonal et al., 2000; Doughty et al., 2014; Janssen et al., 2020a; Stahl et al., 2013). This is confirmed by satellite observations of negative anomalies in sun-induced fluorescence during drought (see also Figure 5b), which is considered a proxy of canopy photosynthesis (Koren et al., 2018; Lee et al., 2013; Yang et al., 2018). The observed decline in leaf-level photosynthesis during the 2015 drought in the central Amazon has been attributed to progressive stomatal closure and not to changes in leaf chemistry (Santos et al., 2018). These results suggest that despite canopy green-up, photosynthesis might well be downregulated during drought because of stomatal limitations (Janssen et al., 2020a; Santos et al., 2018).

560 The analysis of changes in X band vegetation optical depth (VOD) in the area affected by drought in 2005 and 2015 (Figures 4d & 7d) confirms earlier results from passive and active microwave remote sensing studies that showed negative anomalies of VOD and radar backscatter in response to historical droughts in the Amazon basin (van Emmerik et al., 2017; Frohling et al., 2011, 2017; Lee et al., 2013; Liu et al., 2013, 2018b; Saatchi et al., 2013). During the 2015 drought in the central Amazon, van Emmerik *et al.* (2017) found that remotely sensed K_u band radar backscatter declined during the drought which was strongly correlated to *in situ* observed declines in stem girth. In contrast to vegetation indices from multi-spectral remote sensing, passive and active microwave remote sensing is generally sensitive to vegetation biomass and water content and not vegetation greenness (Frappart et al., 2020; Liu et al., 2013; Meesters et al., 2005). Furthermore, X band VOD has been found to be strongly dependent on leaf water potential in temperate forests in North America (Momen et al., 2017). Therefore, the negative anomalies in VOD and radar backscatter in response to drought are likely signalling a decline in vegetation water content during drought (Momen et al., 2017) and can therefore be used as a rough proxy of tree water status and stem growth.

5. Conclusions

Long-term monthly estimates of stem growth, leaf fall and flushing indicate that Amazon green-up during drought is a legacy effect of enhanced leaf flushing at the onset of a drought and cannot be considered a proxy of canopy photosynthesis,



575 aboveground biomass production or forest health in evergreen Neotropical forest. Separating photosynthesis, vegetation water
status and canopy greenness as three sometimes independent properties of the vegetation allows for explaining apparent
discrepancies in drought responses visible in remote sensing data (e.g. Lee et al., 2013; Liu et al., 2018b). To exemplify,
Anderson *et al.* (2010) found that areas that showed the highest EVI green-up during the 2005 drought also experienced the
highest rates of drought-induced tree mortality. Our results also point to a long-term (1982-2019) decline in stem growth rates
580 across the Amazon basin, which appears to be driven by increased warming and drying of the Amazonian climate. While still
uncertain, this decline of carbon sequestration in woody stem growth over time ($-3.04 \cdot 10^{-3} \text{ Mg C ha}^{-1} \text{ yr}^{-2}$) is significantly less
compared to the trend of increasing carbon release through tree mortality ($25.5 \cdot 10^{-3} \text{ Mg C ha}^{-1} \text{ yr}^{-2}$) found in a network of forest
inventory plots (Brienen et al., 2015). As tree mortality is elevated during drought (Feldpausch et al., 2016; Phillips et al.,
2009) it is of critical importance to study the drivers of drought sensitivity and drought-induced tree mortality in Neotropical
585 forest to be able to project future changes in the carbon sink strength of the Amazon basin.

Code availability

The code used in this study will become publicly available after the final revision and publication of this manuscript

Data availability

590 The dataset compiled and analysed in this study will become publicly available after the final revision and publication of this
manuscript

Author contribution

TJ conceived and designed the analysis, collated the dataset, carried out the analysis and wrote the article. YV and BD co-
designed the analysis and have critically reviewed and commented on the article. FH, SL, KN, KF and HD helped with the
writing of the article and have critically reviewed and commented on the article.

595 Competing interests

The authors declare that they have no conflict of interest.

Acknowledgements

We would like to thank all the individual researchers that enabled this study by providing freely available datasets and
accessible figures in addition to their published work. Furthermore we would like to thank Chi Chen for providing us with the



600 most recent version of the Global Data Set of Vegetation Leaf Area Index (LAI3g). We would also like to thank Maurits Kooreman for providing us with the Sun-Induced Fluorescence of Terrestrial Ecosystems Retrieval V2 dataset.

References

- Albert, L. P., Wu, J., Prohaska, N., de Camargo, P. B., Huxman, T. E., Tribuzy, E. S., Ivanov, V. Y., Oliveira, R. S., Garcia, S., Smith, M. N., Oliveira Junior, R. C., Restrepo-Coupe, N., da Silva, R., Stark, S. C., Martins, G. A., Penha, D. V. and Saleska, S. R.: Age-dependent leaf physiology and consequences for crown-scale carbon uptake during the dry season in an Amazon evergreen forest, *New Phytol.*, 219(3), 870–884, doi:10.1111/nph.15056, 2018.
- Andela, N., Liu, Y. Y., M. Van Dijk, A. I. J., De Jeu, R. A. M. and McVicar, T. R.: Global changes in dryland vegetation dynamics (1988–2008) assessed by satellite remote sensing: Comparing a new passive microwave vegetation density record with reflective greenness data, *Biogeosciences*, 10(10), 6657–6676, doi:10.5194/bg-10-6657-2013, 2013.
- 610 Anderson, L. O., Malhi, Y., Arag??o, L. E. O. C., Ladle, R., Arai, E., Barbier, N., Phillips, O., Arag??o, L. E. O. C., Ladle, R., Arai, E., Barbier, N. and Phillips, O.: Remote sensing detection of droughts in Amazonian forest canopies, *New Phytol.*, 187(3), 733–750, doi:10.1111/j.1469-8137.2010.03355.x, 2010.
- Anderson, L. O., Neto, G. R., Cunha, A. P., Fonseca, M. G., Moura, Y. M. De, Dalagnol, R., Wagner, F. H., Eduardo, L., Araga, C. De and Anderson, L. O.: Vulnerability of Amazonian forests to repeated droughts, , doi:10.1098/rstb.2017.0411, 615 2018.
- Arag??o, L. E. O. C., Malhi, Y., Metcalfe, D. B., Silva-Espejo, J. E., Jim??enez, E., Navarrete, D., Almeida, S., Costa, A. C. L., Salinas, N., Phillips, O. L., Anderson, L. O., Baker, T. R., Goncalvez, P. H., Huam??n-Ovalle, J., Mamani-Sol??rzano, M., Meir, P., Monteagudo, A., Pe??uela, M. C., Prieto, A., Quesada, C. A., Rozas-D??vila, A., Rudas, A., Silva Junior, J. A. and V??squez, R.: Above- and below-ground net primary productivity across ten Amazonian forests on contrasting soils, *Biogeosciences*, 620 6(1), 2441–2488, doi:10.5194/bg-6-2441-2009, 2009.
- Asner, G. P. and Alencar, A.: Drought impacts on the Amazon forest: The remote sensing perspective, *New Phytol.*, 187(3), 569–578, doi:10.1111/j.1469-8137.2010.03310.x, 2010.
- Asner, G. P., Townsend, A. R. and Braswell, B. H.: Satellite observation of El Ni??o effects on Amazon forest, *Geophys. Res. Lett.*, 27(7), 981–984, 2000.
- 625 Baker, T. R., Affum-Baffoe, K., Burslem, D. F. R. P. and Swaine, M. D.: Phenological differences in tree water use and the timing of tropical forest inventories: Conclusions from patterns of dry season diameter change, *For. Ecol. Manage.*, 171(3), 261–274, doi:10.1016/S0378-1127(01)00787-3, 2002.
- Banin, L., Lewis, S. L., Lopez-Gonzalez, G., Baker, T. R., Quesada, C. A., Chao, K. J., Burslem, D. F. R. P., Nilus, R., Abu Salim, K., Keeling, H. C., Tan, S., Davies, S. J., Monteagudo Mendoza, A., V??squez, R., Lloyd, J., Neill, D. A., Pitman, N. and Phillips, O. L.: Tropical forest wood production: A cross-continental comparison, *J. Ecol.*, 102(4), 1025–1037, 630 doi:10.1111/1365-2745.12263, 2014.



- Batista, G. T., Shimabukuro, Y. E. and Lawrence, W. T.: The long-term monitoring of vegetation cover in the Amazonian region of northern Brazil using NOAA-AVHRR data, *Int. J. Remote Sens.*, 18(15), 3195–3210, doi:10.1080/014311697217044, 1997.
- 635 Bischl, B., Lang, M., Kotthoff, L., Schratz, P., Schiffner, J., Richter, J., Jones, Z. and Al., E.: Machine Learning in R, [online] Available from: <https://mlr.mlr-org.com>, 2020.
- Boisier, J. P., Ciais, P., Ducharne, A. and Guimberteau, M.: Projected strengthening of Amazonian dry season by constrained climate model simulations, *Nat. Clim. Chang.*, 5(7), 656–660, doi:10.1038/nclimate2658, 2015.
- Bonal, D., Barigah, T. S., Granier, A. and Guehl, J. M.: Late-stage canopy tree species with extremely low $\delta^{13}\text{C}$ and high stomatal sensitivity to seasonal soil drought in the tropical rainforest of French Guiana, *Plant, Cell Environ.*, 23(5), 445–459, doi:10.1046/j.1365-3040.2000.00556.x, 2000.
- 640 Bonal, D., Bosc, A., Ponton, S., Goret, J. Y., Burban, B. T., Gross, P., Bonnefond, J. M., Elbers, J., Longdoz, B., Epron, D., Guehl, J. M. and Granier, A.: Impact of severe dry season on net ecosystem exchange in the Neotropical rainforest of French Guiana, *Glob. Chang. Biol.*, 14(8), 1917–1933, doi:10.1111/j.1365-2486.2008.01610.x, 2008.
- 645 Borchert, R.: Water status and development of tropical trees during seasonal drought, *Trees*, 8(3), 115–125, doi:10.1007/BF00196635, 1994.
- Borchert, R., Rivera, G. and Hagnauer, W.: Modification of vegetative phenology in a tropical semi-deciduous forest by abnormal drought and rain, *Biotropica*, 34(1), 27–39, doi:10.1111/j.1744-7429.2002.tb00239.x, 2002.
- Borchert, R., Calle, Z., Strahler, A. H., Baertschi, A., Magill, R. E., Broadhead, J. S., Kamau, J., Njoroge, J. and Muthuri, C.: 650 Insolation and photoperiodic control of tree development near the equator, *New Phytol.*, 205(1), 7–13, doi:10.1111/nph.12981, 2015.
- Brienen, R. J. W., Phillips, O. L., Feldpausch, T. R., Gloor, E., Baker, T. R., Lloyd, J., Lopez-Gonzalez, G., Monteagudo-Mendoza, A., Malhi, Y., Lewis, S. L., Vásquez Martínez, R., Alexiades, M., Álvarez Dávila, E., Alvarez-Loayza, P., Andrade, A., Aragaõ, L. E. O. C., Araujo-Murakami, A., Arets, E. J. M. M., Arroyo, L., Aymard C., G. A., Bánki, O. S., Baraloto, C., 655 Barroso, J., Bonal, D., Boot, R. G. A., Camargo, J. L. C., Castilho, C. V., Chama, V., Chao, K. J., Chave, J., Comiskey, J. A., Cornejo Valverde, F., Da Costa, L., De Oliveira, E. A., Di Fiore, A., Erwin, T. L., Fauset, S., Forsthofer, M., Galbraith, D. R., Grahame, E. S., Groot, N., Hérault, B., Higuchi, N., Honorio Coronado, E. N., Keeling, H., Killeen, T. J., Laurance, W. F., Laurance, S., Licona, J., Magnussen, W. E., Marimon, B. S., Marimon-Junior, B. H., Mendoza, C., Neill, D. A., Nogueira, E. M., Núñez, P., Pallqui Camacho, N. C., Parada, A., Pardo-Molina, G., Peacock, J., Penã-Claros, M., Pickavance, G. C., Pitman, 660 N. C. A., Poorter, L., Prieto, A., Quesada, C. A., Ramírez, F., Ramírez-Angulo, H., Restrepo, Z., Roopsind, A., Rudas, A., Salomaõ, R. P., Schwarz, M., Silva, N., Silva-Espejo, J. E., Silveira, M., Stropp, J., Talbot, J., Ter Steege, H., Teran-Aguilar, J., Terborgh, J., Thomas-Caesar, R., Toledo, M., Torello-Raventos, M., Umetsu, R. K., Van Der Heijden, G. M. F., Van Der Hout, P., Guimarães Vieira, I. C., Vieira, S. A., Vilanova, E., Vos, V. A. and Zagt, R. J.: Long-term decline of the Amazon carbon sink, *Nature*, 519(7543), 344–348, doi:10.1038/nature14283, 2015.
- 665 Butler, E. E., Datta, A., Flores-Moreno, H., Chen, M., Wythers, K. R., Fazayeli, F., Banerjee, A., Atkin, O. K., Kattge, J.,



- Amiaud, B., Blonder, B., Boenisch, G., Bond-Lamberty, B., Brown, K. A., Byun, C., Campetella, G., Cerabolini, B. E. L., Cornelissen, J. H. C., Craine, J. M., Craven, D., de Vries, F. T., Díaz, S., Domingues, T. F., Forey, E., González-Melo, A., Gross, N., Han, W., Hattingh, W. N., Hickler, T., Jansen, S., Kramer, K., Kraft, N. J. B., Kurokawa, H., Laughlin, D. C., Meir, P., Minden, V., Niinemets, Ü., Onoda, Y., Peñuelas, J., Read, Q., Sack, L., Schamp, B., Soudzilovskaia, N. A., Spasojevic, M.
- 670 J., Sosinski, E., Thornton, P. E., Valladares, F., van Bodegom, P. M., Williams, M., Wirth, C. and Reich, P. B.: Mapping local and global variability in plant trait distributions, *Proc. Natl. Acad. Sci.*, 201708984, doi:10.1073/pnas.1708984114, 2017.
- Chave, J., Navarrete, D., Almeida, S., Álvarez, E., Aragão, L. E. O. C., Bonal, D., Châtelet, P., Silva Espejo, J., Goret, J.-Y., von Hildebrand, P., Jiménez, E., Patiño, S., Peñuela, M. C., Phillips, O. L., Stevenson, P. and Malhi, Y.: Regional and temporal patterns of litterfall in tropical South America, *Biogeosciences Discuss.*, 6, 7565–7597, doi:10.5194/bgd-6-7565-2009, 2009.
- 675 Chave, J., Navarrete, D., Almeida, S., Álvarez, E., Aragão, L. E. O. C., Bonal, D., Châtelet, P., Silva-Espejo, J. E., Goret, J. Y., Von Hildebrand, P., Jiménez, E., Patiño, S., Peñuela, M. C., Phillips, O. L., Stevenson, P. and Malhi, Y.: Regional and seasonal patterns of litterfall in tropical South America, *Biogeosciences*, 7(1), 43–55, doi:10.5194/bg-7-43-2010, 2010.
- Chen, T. and Guestrin, C.: XGBoost: A scalable tree boosting system, *Proc. ACM SIGKDD Int. Conf. Knowl. Discov. Data Min.*, 13-17-Aug, 785–794, doi:10.1145/2939672.2939785, 2016.
- 680 Chen, T., He, T., Benesty, M., Khotilovich, V., Tang, Y., Cho, H., Chen, K., Mitchell, R., Cano, I., Zhou, T., Li, M., Xie, J., Lin, M., Geng, Y. and Li, Y.: Extreme Gradient Boosting, *Packag. ‘xgboost,’* doi:10.1145/2939672.2939785, 2020.
- Clark, D. A., Piper, S. C., Keeling, C. D. and Clark, D. B.: Tropical rain forest tree growth and atmospheric carbon dynamics linked to interannual temperature variation during 1984-2000, *Proc. Natl. Acad. Sci.*, 100(10), 5852–5857, doi:10.1073/pnas.0935903100, 2003.
- 685 Cox, P. M., Harris, P. P., Huntingford, C., Betts, R. A., Collins, M., Jones, C. D., Jupp, T. E., Marengo, J. A. and Nobre, C. A.: Increasing risk of Amazonian drought due to decreasing aerosol pollution, *Nature*, 453(7192), 212–215, doi:10.1038/nature06960, 2008.
- Dessay, N., Laurent, H., Machado, L. A. T., Shimabukuro, Y. E., Batista, G. T., Diedhiou, A. and Ronchail, J.: Comparative study of the 1982-1983 and 1997-1998 El Niño events over different types of vegetation in South America, *Int. J. Remote*
- 690 *Sens.*, 25(20), 4063–4077, doi:10.1080/0143116031000101594, 2004.
- Detto, M., Wright, S. J., Calderón, O. and Muller-Landau, H. C.: Resource acquisition and reproductive strategies of tropical forest in response to the El Niño-Southern Oscillation, *Nat. Commun.*, 9(1), 1–8, doi:10.1038/s41467-018-03306-9, 2018.
- Dias, D. P. and Marengo, R. A.: Tree growth, wood and bark water content of 28 Amazonian tree species in response to variations in rainfall and wood density, *IForest*, 9(JUNE2016), 445–451, doi:10.3832/ifor1676-008, 2016.
- 695 Didan, K.: MOD13C1 MODIS/Terra Vegetation Indices 16-Day L3 Global 0.05Deg CMG V006., 2015.
- Doughty, C. E. and Goulden, M. L.: Seasonal patterns of tropical forest leaf area index and CO₂ exchange, *J. Geophys. Res. Biogeosciences*, 114(1), n/a-n/a, doi:10.1029/2007JG000590, 2009.
- Doughty, C. E., Malhi, Y., Araujo-murakami, A., Metcalfe, D. B., Silva-Espejo, J. E., Arroyo, L., Heredia, J. P., Pardo-Toledo, E., Mendizabal, L. M., Rojas-Landivar, V. D., Vega-Martinez, M., Flores-Valencia, M., Sibling-Rivero, R., Moreno-Vare, L.,



- 700 Jessica Viscarra, L., Chuviru-Castro, T., Osinaga-Becerra, M., Ledezma, R., Javier, E., Arroyo, L., Heredia, J. P., Pardo-Toledo, E., Mendizabal, L. M. and Victor, D.: Allocation trade-offs dominate the response of tropical forest growth to seasonal and interannual drought, *Ecology*, 95(8), 1–6, doi:10.1890/13-1507.1, 2014.
- Doughty, C. E., Metcalfe, D. B., Girardin, C. A. J., Amézquita, F. F., Cabrera, D. G., Huasco, W. H., Silva-Espejo, J. E., Araujo-Murakami, A., da Costa, M. C., Rocha, W., Feldpausch, T. R., Mendoza, A. L. M., da Costa, A. C. L., Meir, P., Phillips,
705 O. L. and Malhi, Y.: Drought impact on forest carbon dynamics and fluxes in Amazonia, *Nature*, 519(7541), 78–82, doi:10.1038/nature14213, 2015a.
- Doughty, C. E., Metcalfe, D. B., Girardin, C. a J., Amezquita, F. F., Durand, L., Huasco, W. H., Costa, M. C., Costa, a C. L., Rocha, W., Meir, P., Galbraith, D. and Malhi, Y.: Source and sink carbon dynamics and carbon allocation in the Amazon basin, *Global Biogeochem. Cycles*, 1–11, doi:10.1002/2014GB005028. Received, 2015b.
- 710 ECMWF: ERA5 | ECMWF, ERA5 [online] Available from: <https://www.ecmwf.int/en/forecasts/datasets/reanalysis-datasets/era5> (Accessed 25 October 2019), 2019.
- Elliott, S., Baker, P. J. and Borchert, R.: Leaf flushing during the dry season: the paradox of Asian monsoon forests, *Glob. Ecol. Biogeogr.*, 15(3), 248–257, doi:10.1111/j.1466-822x.2006.00213.x, 2006.
- van Emmerik, T., Steele-Dunne, S. C., Paget, A., Oliveira, R. S. de, Bittencourt, P. R. L. L., Barros, F. de V., van de Giesen,
715 N., Giesen, N. van de and van de Giesen, N.: Water stress detection in the Amazon using radar, *Geophys. Res. Lett.*, 44(13), 6841–6849, doi:10.1002/2017GL073747, 2017.
- Fan, J., Yue, W., Wu, L., Zhang, F., Cai, H., Wang, X., Lu, X. and Xiang, Y.: Evaluation of SVM, ELM and four tree-based ensemble models for predicting daily reference evapotranspiration using limited meteorological data in different climates of China, *Agric. For. Meteorol.*, 263(July), 225–241, doi:10.1016/j.agrformet.2018.08.019, 2018.
- 720 Feldpausch, T. R., Lloyd, J., Lewis, S. L., Brienen, R. J. W., Gloor, M., Monteagudo Mendoza, A., Lopez-Gonzalez, G., Banin, L., Abu Salim, K., Affum-Baffoe, K., Alexiades, M., Almeida, S., Amaral, I., Andrade, A., Aragão, L. E. O. C., Araujo Murakami, A., Arets, E. J. M., Arroyo, L., Aymard C., G. A., Baker, T. R., Bánki, O. S., Berry, N. J., Cardozo, N., Chave, J., Comiskey, J. A., Alvarez, E., De Oliveira, A., Di Fiore, A., Djagbletey, G., Domingues, T. F., Erwin, T. L., Fearnside, P. M., França, M. B., Freitas, M. A., Higuchi, N., Honorio C., E., Iida, Y., Jiménez, E., Kassim, A. R., Killeen, T. J., Laurance, W.
725 F., Lovett, J. C., Malhi, Y., Marimon, B. S., Marimon-Junior, B. H., Lenza, E., Marshall, A. R., Mendoza, C., Metcalfe, D. J., Mitchard, E. T. A., Neill, D. A., Nelson, B. W., Nilus, R., Nogueira, E. M., Parada, A., S.-H. Peh, K., Pena Cruz, A., Peñuela, M. C., Pitman, N. C. A., Prieto, A., Quesada, C. A., Ramírez, F., Ramírez-Angulo, H., Reitsma, J. M., Rudas, A., Saiz, G., Salomão, R. P., Schwarz, M., Silva, N., Silva-Espejo, J. E., Silveira, M., Sonké, B., Stropp, J., Taedoumg, H. E., Tan, S., Ter Steege, H., Terborgh, J., Torello-Raventos, M., Van Der Heijden, G. M. F., Vásquez, R., Vilanova, E., Vos, V. A., White, L.,
730 Willcock, S., Woell, H. and Phillips, O. L.: Tree height integrated into pantropical forest biomass estimates, *Biogeosciences*, 9(8), 3381–3403, doi:10.5194/bg-9-3381-2012, 2012.
- Feldpausch, T. R., Phillips, O. L., Brienen, R. J. W., Gloor, E., Lloyd, J., Malhi, Y., Alarcón, A., Dávila, E. Á., Andrade, A., Aragao, L. E. O. C., Arroyo, L., Aymard, G. A. C., Baker, T. R., Baraloto, C., Barroso, J., Bonal, D., Castro, W., Chama, V.,



- Chave, J., Domingues, T. F., Fauset, S., Groot, N., Coronado, E. H., Laurance, S., Laurance, W. F., Lewis, S. L., Licona, J. C.,
735 Marimon, B. S., Bautista, C. M., Neill, D. A., Oliveira, E. A., Santos, C. O., Camacho, N. C. P., Prieto, A., Quesada, C. A.,
Ramírez, F., Rudas, A., Saiz, G., Salomão, R. P., Silveira, M., Steege, H., Stropp, J., Terborgh, J., Heijden, G. M. F., Martinez,
R. V., Vilanova, E. and Vos, V. A.: Amazon forest response to repeated droughts, *Global Biogeochem. Cycles*, 30(7), 964–
982, doi:10.1002/2015GB005133. Received, 2016.
- Fleischer, K., Rammig, A., De Kauwe, M. G., Walker, A. P., Domingues, T. F., Fuchslueger, L., Garcia, S., Goll, D. S.,
740 Grandis, A., Jiang, M., Haverd, V., Hofhansl, F., Holm, J. A., Kruijt, B., Leung, F., Medlyn, B. E., Mercado, L. M., Norby, R.
J., Pak, B., von Randow, C., Quesada, C. A., Schaap, K. J., Valverde-Barrantes, O. J., Wang, Y.-P., Yang, X., Zaehle, S., Zhu,
Q. and Lapola, D. M.: Amazon forest response to CO₂ fertilization dependent on plant phosphorus acquisition, *Nat. Geosci.*,
12(9), 736–741, doi:10.1038/s41561-019-0404-9, 2019.
- Frappart, F., Wigneron, J. P., Li, X., Liu, X., Al-Yaari, A., Fan, L., Wang, M., Moisy, C., Le Masson, E., Lafkih, Z. A., Vallé,
745 C., Ygorra, B. and Baghdadi, N.: Global monitoring of the vegetation dynamics from the vegetation optical depth (VOD): A
review, *Remote Sens.*, 12(18), 7–10, doi:10.3390/RS12182915, 2020.
- Frolking, S., Milliman, T., Palace, M., Wisser, D., Lammers, R. and Fahnestock, M.: Tropical forest backscatter anomaly
evident in SeaWinds scatterometer morning overpass data during 2005 drought in Amazonia, *Remote Sens. Environ.*, 115(3),
897–907, doi:10.1016/j.rse.2010.11.017, 2011.
- 750 Frolking, S., Hagen, S., Braswell, B., Milliman, T., Herrick, C., Peterson, S., Roberts, D., Keller, M. and Palace, M.: Evaluating
multiple causes of persistent low microwave backscatter from Amazon forests after the 2005 drought, *PLoS One*, 12(9), 1–22,
doi:10.1371/journal.pone.0183308, 2017.
- Fu, R., Yin, L., Li, W., Arias, P. A., Dickinson, R. E., Huang, L., Chakraborty, S., Fernandes, K., Liebmann, B., Fisher, R. and
Myneni, R. B.: Increased dry-season length over southern Amazonia in recent decades and its implication for future climate
755 projection, *Proc. Natl. Acad. Sci.*, 110(45), 18110–18115, doi:10.1073/pnas.1302584110, 2013.
- Gao, X., Huete, A. R., Ni, W. and Miura, T.: Optical-biophysical relationships of vegetation spectra without background
contamination, *Remote Sens. Environ.*, 74(3), 609–620, doi:10.1016/S0034-4257(00)00150-4, 2000.
- Girardin, C. A. J. C. A. J. C. A. J., Malhi, Y., Doughty, C. E., Metcalfe, D. B., Meir, P., Aguila-Pasquel, J., Araujo-Murakami,
A., Costa, A. C. L., Silva-Espejo, J. E., Amézquita, F. F., Rowland, L., del Aguila-Pasquel, J., Araujo-Murakami, A., da Costa,
760 A. C. L., Silva-Espejo, J. E., Farfı̃n Amı̃zquita, F., Rowland, L., Aguila-Pasquel, J., Araujo-Murakami, A., Costa, A. C.
L., Silva-Espejo, J. E., Amézquita, F. F. and Rowland, L.: Seasonal trends of Amazonian rainforest phenology, net primary
productivity, and carbon allocation, *Global Biogeochem. Cycles*, 30(5), 700–715, doi:10.1002/2015GB005270. Received,
2016.
- Gonçalves, N. B., Lopes, A. P., Dalagnol, R., Wu, J., Pinho, D. M. and Nelson, B. W.: Both near-surface and satellite remote
765 sensing confirm drought legacy effect on tropical forest leaf phenology after 2015/2016 ENSO drought, *Remote Sens.
Environ.*, 237(September 2019), 111489, doi:10.1016/j.rse.2019.111489, 2020.
- Guyon, I. and Elisseeff, A.: An Introduction to Variable and Feature Selection Isabelle, *J. Mach. Learn. Res.*, 3, 1157–1182,



- 2003.
- Heineman, K. D., Caballero, P., Morris, A., Velasquez, C., Serrano, K., Ramos, N., Gonzalez, J., Mayorga, L., Corre, M. D.
770 and Dalling, J. W.: Variation in canopy litterfall along a precipitation and soil fertility gradient in a panamanian lower montane
forest, *Biotropica*, 47(3), 300–309, doi:10.1111/btp.12214, 2015.
- Hengl, T., De Jesus, J. M., Heuvelink, G. B. M., Gonzalez, M. R., Kilibarda, M., Blagotić, A., Shangguan, W., Wright, M. N.,
Geng, X., Bauer-Marschallinger, B., Guevara, M. A., Vargas, R., MacMillan, R. A., Batjes, N. H., Leenaars, J. G. B., Ribeiro,
E., Wheeler, I., Mantel, S. and Kempen, B.: SoilGrids250m: Global gridded soil information based on machine learning., 2017.
- 775 Hofhansl, F., Kobler, J., Ofner, J., Drage, S., Pölz, E. M. and Wanek, W.: Sensitivity of tropical forest aboveground
productivity to climate anomalies in SW Costa Rica, *Global Biogeochem. Cycles*, 28(12), 1437–1454,
doi:10.1002/2014GB004934, 2014.
- Hofhansl, F., Org Schnecker, J., Singer, G. and Wanek, W.: New insights into mechanisms driving carbon allocation in tropical
forests, *New Phytol.*, 205, 137–146, doi:10.1111/nph.13007, 2015.
- 780 Hofhansl, F., Andersen, K. M., Fleischer, K., Fuchslueger, L., Rammig, A., Schaap, K. J., Valverde-Barrantes, O. J. and
Lapola, D. M.: Amazon Forest Ecosystem Responses to Elevated Atmospheric CO₂ and Alterations in Nutrient Availability:
Filling the Gaps with Model-Experiment Integration, *Front. Earth Sci.*, 4(February), 1–9, doi:10.3389/feart.2016.00019, 2016.
- Hofhansl, F., Chacón-Madrigal, E., Fuchslueger, L., Jenking, D., Morera-Beita, A., Plutzer, C., Silla, F., Andersen, K. M.,
Buchs, D. M., Dullinger, S., Fiedler, K., Franklin, O., Hietz, P., Huber, W., Quesada, C. A., Rammig, A., Schrod, F., Vincent,
785 A. G., Weissenhofer, A. and Wanek, W.: Climatic and edaphic controls over tropical forest diversity and vegetation carbon
storage, *Sci. Rep.*, 10(1), 1–11, doi:10.1038/s41598-020-61868-5, 2020.
- Holm, J. A., Knox, R. G., Zhu, Q., Fisher, R. A., Koven, C. D., Nogueira Lima, A. J., Riley, W. J., Longo, M., Negrón-Juárez,
R. I., de Araujo, A. C., Kueppers, L. M., Moorcroft, P. R., Higurashi, N. and Chambers, J. Q.: The Central Amazon Biomass
Sink Under Current and Future Atmospheric CO₂: Predictions From Big-Leaf and Demographic Vegetation Models, *J.*
790 *Geophys. Res. Biogeosciences*, 125(3), 1–23, doi:10.1029/2019JG005500, 2020.
- Hubau, W., Lewis, S. L., Phillips, O. L., Affum-Baffoe, K., Beekman, H., Cuní-Sánchez, A., Daniels, A. K., Ewango, C. E.
N., Fauset, S., Mukinzi, J. M., Sheil, D., Sonké, B., Sullivan, M. J. P., Sunderland, T. C. H., Taedoumg, H., Thomas, S. C.,
White, L. J. T., Abernethy, K. A., Adu-Bredu, S., Amani, C. A., Baker, T. R., Banin, L. F., Baya, F., Begne, S. K., Bennett,
A. C., Benedet, F., Bitariho, R., Bocko, Y. E., Boeckx, P., Boundja, P., Brienen, R. J. W., Brncic, T., Chezeaux, E., Chuyong,
795 G. B., Clark, C. J., Collins, M., Comiskey, J. A., Coomes, D. A., Dargie, G. C., de Haulleville, T., Kamdem, M. N. D., Doucet,
J. L., Esquivel-Muelbert, A., Feldpausch, T. R., Fofanah, A., Foli, E. G., Gilpin, M., Gloor, E., Gonmadje, C., Gourlet-Fleury,
S., Hall, J. S., Hamilton, A. C., Harris, D. J., Hart, T. B., Hockemba, M. B. N., Hladik, A., Ifo, S. A., Jeffery, K. J., Jucker, T.,
Yakusu, E. K., Kearsley, E., Kenfack, D., Koch, A., Leal, M. E., Levesley, A., Lindsell, J. A., Lisingo, J., Lopez-Gonzalez,
G., Lovett, J. C., Makana, J. R., Malhi, Y., Marshall, A. R., Martin, J., Martin, E. H., Mbayu, F. M., Medjibe, V. P., Mihindou,
800 V., Mitchard, E. T. A., Moore, S., Munishi, P. K. T., Bengone, N. N., Ojo, L., Ondo, F. E., Peh, K. S. H., Pickavance, G. C.,
Poulsen, A. D., Poulsen, J. R., Qie, L., Reitsma, J., Rovero, F., Swaine, M. D., Talbot, J., Taplin, J., Taylor, D. M., Thomas,



- D. W., Toirambe, B., Mukendi, J. T., Tuagben, D., Umunay, P. M., et al.: Asynchronous carbon sink saturation in African and Amazonian tropical forests, *Nature*, 579(7797), 80–87, doi:10.1038/s41586-020-2035-0, 2020.
- Huete, A., Didan, K., Shimabokuro, Y., Ferreira, L. and Rodriguez, E.: Regional amazon basin and global analyses of MODIS
805 vegetation indices: Early results and comparisons with AVHRR, in *International Geoscience and Remote Sensing Symposium (IGARSS)*, vol. 2, pp. 536–538., 2000.
- Jackson, T. J. and Schmugge, T. J.: Vegetation effects on the microwave emission of soils, *Remote Sens. Environ.*, 36(3), 203–212, doi:10.1016/0034-4257(91)90057-D, 1991.
- Janssen, T., Fleischer, K., Luysaert, S., Naudts, K. and Dolman, H.: Drought resistance increases from the individual to the
810 ecosystem level in highly diverse Neotropical rainforest: a meta-analysis of leaf, tree and ecosystem responses to drought, *Biogeosciences*, 17(9), 2621–2645, doi:10.5194/bg-17-2621-2020, 2020a.
- Janssen, T. A. J., Hölttä, T., Fleischer, K., Naudts, K. and Dolman, H.: Wood allocation trade-offs between fiber wall, fiber lumen, and axial parenchyma drive drought resistance in neotropical trees, *Plant. Cell Environ.*, 43(4), 965–980, doi:10.1111/pce.13687, 2020b.
- 815 Jiménez-Muñoz, J. C., Mattar, C., Barichivich, J., Santamaría-Artigas, A., Takahashi, K., Malhi, Y., Sobrino, J. A. and Schrier, G. van der: Record-breaking warming and extreme drought in the Amazon rainforest during the course of El Niño 2015–2016, *Sci. Rep.*, 6, 33130, doi:10.1038/srep33130, 2016.
- Jones, M. O., Jones, L. A., Kimball, J. S. and McDonald, K. C.: Satellite passive microwave remote sensing for monitoring global land surface phenology, *Remote Sens. Environ.*, 115(4), 1102–1114, doi:10.1016/j.rse.2010.12.015, 2011.
- 820 Jones, M. O., Kimball, J. S. and Nemani, R. R.: Asynchronous Amazon forest canopy phenology indicates adaptation to both water and light availability, *Environ. Res. Lett.*, 9(12), 124021, doi:10.1088/1748-9326/9/12/124021, 2014.
- Kitajima, K., Mulkey, S. S., Samaniego, M. and Wright, S. J.: Decline of photosynthetic capacity with leaf age and position in two tropical pioneer tree species, *Am. J. Bot.*, 89(12), 1925–1932, doi:10.3732/ajb.89.12.1925, 2002.
- Koren, G., Van Schaik, E., Araújo, A. C., Boersma, K. F., Gärtner, A., Killaars, L., Kooreman, M. L., Kruijt, B., Van Der
825 Laan-Luijkx, I. T., Von Randow, C., Smith, N. E. and Peters, W.: Widespread reduction in sun-induced fluorescence from the Amazon during the 2015/2016 El Niño, *Philos. Trans. R. Soc. B Biol. Sci.*, 373(1760), doi:10.1098/rstb.2017.0408, 2018.
- Körner, C. and Basel, M. L.: Growth Controls Photosynthesis – Mostly, *Nov. Acta Leopoldina*, 283(391), 273–283 [online] Available from:
https://www.researchgate.net/profile/Christian_Koerner3/publication/236680450_Growth_controls_photosynthesis-Mostly/links/0a85e52fbd7e614407000000.pdf (Accessed 24 January 2018), 2013.
- 830 Lapola, D. M., Oyama, M. D. and Nobre, C. A.: Exploring the range of climate biome projections for tropical South America: The role of CO₂ fertilization and seasonality, *Global Biogeochem. Cycles*, 23(3), 1–16, doi:10.1029/2008GB003357, 2009.
- Lee, J.-E., Frankenberg, C., van der Tol, C., Berry, J. A., Guanter, L., Boyce, C. K., Fisher, J. B., Morrow, E., Worden, J. R., Asefi, S., Badgley, G. and Saatchi, S.: Forest productivity and water stress in Amazonia: observations from GOSAT
835 chlorophyll fluorescence, *Proc. R. Soc. B Biol. Sci.*, 280(1761), 20130171–20130171, doi:10.1098/rspb.2013.0171, 2013.



- Liu, X., Zeng, X., Zou, X., González, G., Wang, C. and Yang, S.: Litterfall production prior to and during Hurricanes Irma and Maria in four puerto Rican forests, *Forests*, 9(6), doi:10.3390/f9060367, 2018a.
- Liu, Y., de Jeu, R. A. M., van Dijk, A. I. J. M. and Owe, M.: TRMM-TMI satellite observed soil moisture and vegetation density (1998–2005) show strong connection with El Niño in eastern Australia, *Geophys. Res. Lett.*, 34(15),
840 doi:10.1029/2007GL030311, 2007.
- Liu, Y. Y., van Dijk, A. I. J. M., McCabe, M. F., Evans, J. P. and de Jeu, R. A. M.: Global vegetation biomass change (1988–2008) and attribution to environmental and human drivers, *Glob. Ecol. Biogeogr.*, 22(6), 692–705, doi:10.1111/geb.12024, 2013.
- Liu, Y. Y., van Dijk, A. I. J. M. J. M., de Jeu, R. A. M. M., Canadell, J. G., McCabe, M. F., Evans, J. P. and Wang, G.: Recent
845 reversal in loss of global terrestrial biomass, *Nat. Clim. Chang.*, 5(5), 470–474, doi:10.1038/nclimate2581, 2015.
- Liu, Y. Y., van Dijk, A. I. J. M., Miralles, D. G., McCabe, M. F., Evans, J. P., de Jeu, R. A. M., Gentine, P., Huete, A., Parinussa, R. M., Wang, L., Guan, K., Berry, J. and Restrepo-Coupe, N.: Enhanced canopy growth precedes senescence in 2005 and 2010 Amazonian droughts, *Remote Sens. Environ.*, 211(September 2017), 26–37, doi:10.1016/j.rse.2018.03.035, 2018b.
- 850 Malhi, Y., Aragão, L. E. O. C., Metcalfe, D. B., Paiva, R., Quesada, C. A., Almeida, S., Anderson, L., Brando, P., Chambers, J. Q., da Costa, A. C. L., Hutrya, L. R., Oliveira, P., Patiño, S., Pyle, E. H., Robertson, A. L. and Teixeira, L. M.: Comprehensive assessment of carbon productivity, allocation and storage in three Amazonian forests, *Glob. Chang. Biol.*, 15(5), 1255–1274, doi:10.1111/j.1365-2486.2008.01780.x, 2009a.
- Malhi, Y., Aragao, L. E. O. C., Galbraith, D., Huntingford, C., Fisher, R., Zelazowski, P., Sitch, S., McSweeney, C. and Meir,
855 P.: Exploring the likelihood and mechanism of a climate-change-induced dieback of the Amazon rainforest, *Proc. Natl. Acad. Sci.*, 106(49), 20610–20615, doi:10.1073/pnas.0804619106, 2009b.
- Marengo, J. A., Ambrizzi, T., da Rocha, R. P., Alves, L. M., Cuadra, S. V., Valverde, M. C., Torres, R. R., Santos, D. C. and Ferraz, S. E. T.: Future change of climate in South America in the late twenty-first century: Intercomparison of scenarios from three regional climate models, *Clim. Dyn.*, 35(6), 1089–1113, doi:10.1007/s00382-009-0721-6, 2010.
- 860 Marengo, J. A., Tomasella, J., Alves, L. M., Soares, W. R. and Rodriguez, D. A.: The drought of 2010 in the context of historical droughts in the Amazon region, *Geophys. Res. Lett.*, 38(12), doi:10.1029/2011GL047436, 2011.
- van Marle, M. J. E., van der Werf, G. R., de Jeu, R. a. M. and Liu, Y. Y.: Annual South American forest loss estimates based on passive microwave remote sensing (1990–2010), *Biogeosciences*, 13(2), 609–624, doi:10.5194/bg-12-11499-2015, 2016.
- Meesters, A. G. C. A., De Jeu, R. A. M. and Owe, M.: Analytical derivation of the vegetation optical depth from the microwave polarization difference index, *IEEE Geosci. Remote Sens. Lett.*, 2(2), 121–123, doi:10.1109/LGRS.2005.843983, 2005.
- 865 Meinzer, F. C., James, S. A., Goldstein, G. and Woodruff, D.: Whole-tree water transport scales with sapwood capacitance in tropical forest canopy trees, *Plant, Cell Environ.*, 26(7), 1147–1155, doi:10.1046/j.1365-3040.2003.01039.x, 2003.
- Mitchard, E. T. A., Saatchi, S. S., Gerard, F. F., Lewis, S. L. and Meir, P.: Measuring woody encroachment along a forest-savanna boundary in Central Africa, *Earth Interact.*, 13(8), doi:10.1175/2009EI278.1, 2009a.



- 870 Mitchard, E. T. A., Saatchi, S. S., Woodhouse, I. H., Nangendo, G., Ribeiro, N. S., Williams, M., Ryan, C. M., Lewis, S. L.,
Feldpausch, T. R. and Meir, P.: Using satellite radar backscatter to predict above-ground woody biomass: A consistent
relationship across four different African landscapes, *Geophys. Res. Lett.*, 36(23), 1–6, doi:10.1029/2009GL040692, 2009b.
Moesinger, L., Dorigo, W., De Jeu, R., Van Der Schalie, R., Scanlon, T., Teubner, I. and Forkel, M.: The global long-term
microwave Vegetation Optical Depth Climate Archive (VODCA), *Earth Syst. Sci. Data*, 12(1), 177–196, doi:10.5194/essd-
875 12-177-2020, 2020.
- Momen, M., Wood, J. D., Novick, K. A., Pangle, R., Pockman, W. T., McDowell, N. G. and Konings, A. G.: Interacting
Effects of Leaf Water Potential and Biomass on Vegetation Optical Depth, *J. Geophys. Res. Biogeosciences*, 122(11), 3031–
3046, doi:10.1002/2017JG004145, 2017.
- Muller, B., Pantin, F., Génard, M., Turc, O., Freixes, S., Piques, M. and Gibon, Y.: Water deficits uncouple growth from
880 photosynthesis, increase C content, and modify the relationships between C and growth in sink organs, *J. Exp. Bot.*, 62(6),
1715–1729, doi:10.1093/jxb/erq438, 2011.
- Oliva Carrasco, L., Bucci, S. J., Di Francescantonio, D., Lezcano, O. A., Campanello, P. I., Scholz, F. G., Rodriguez, S.,
Madanes, N., Cristiano, P. M., Hao, G. Y. G.-Y., Holbrook, N. M., Goldstein, G., Rodríguez, S., Madanes, N., Cristiano, P.
M., Hao, G. Y. G.-Y., Holbrook, N. M. and Goldstein, G.: Water storage dynamics in the main stem of subtropical tree species
885 differing in wood density, growth rate and life history traits, *Tree Physiol.*, 35(4), 354–365, doi:10.1093/treephys/tpu087,
2015.
- Owe, M., De Jeu, R. and Walker, J.: A methodology for surface soil moisture and vegetation optical depth retrieval using the
microwave polarization difference index, *IEEE Trans. Geosci. Remote Sens.*, 39(8), 1643–1654, doi:10.1109/36.942542,
2001.
- 890 Pan, Y., Birdsey, R. A., Fang, J., Houghton, R., Kauppi, P. E., Kurz, W. A., Phillips, O. L., Shvidenko, A., Lewis, S. L.,
Canadell, J. G., Ciais, P., Jackson, R. B., Pacala, S. W., McGuire, A. D., Piao, S., Rautiainen, A., Sitch, S. and Hayes, D.: A
large and persistent carbon sink in the world’s forests, *Science (80-.)*, 333(6045), 988–993, doi:10.1126/science.1201609,
2011.
- Phillips, O. L., Lewis, S. L., Baker, T. R., Chao, K.-J. and Higuchi, N.: The changing Amazon forest, *Philos. Trans. R. Soc. B*
895 *Biol. Sci.*, 363(1498), 1819–1827, doi:10.1098/rstb.2007.0033, 2008.
- Phillips, O. L., Aragão, L. E. O. C., Lewis, S. L., Fisher, J. B., Lloyd, J., López-González, G., Malhi, Y., Monteagudo, A.,
Peacock, J., Quesada, C. A., Van Der Heijden, G., Almeida, S., Amaral, I., Arroyo, L., Aymard, G., Baker, T. R., Bánki, O.,
Blanc, L., Bonal, D., Brando, P., Chave, J., De Oliveira, Á. C. A., Cardozo, N. D., Czimczik, C. I., Feldpausch, T. R., Freitas,
M. A., Gloor, E., Higuchi, N., Jiménez, E., Lloyd, G., Meir, P., Mendoza, C., Morel, A., Neill, D. A., Nepstad, D., Patiño, S.,
900 Peñuela, M. C., Prieto, A., Ramírez, F., Schwarz, M., Silva, J., Silveira, M., Thomas, A. S., Steege, H. Ter, Stropp, J., Vásquez,
R., Zelazowski, P., Dávila, E. A., Andelman, S., Andrade, A., Chao, K. J., Erwin, T., Di Fiore, A., Honorio, E. C., Keeling,
H., Killeen, T. J., Laurance, W. F., Cruz, A. P., Pitman, N. C. A., Vargas, P. N., Ramírez-Angulo, H., Rudas, A., Salamão, R.,
Silva, N., Terborgh, J. and Torres-Lezama, A.: Drought sensitivity of the amazon rainforest, *Science (80-.)*, 323(5919), 1344–



- 1347, doi:10.1126/science.1164033, 2009.
- 905 Phillips, O. L., Brienen, R. J. W., Gloor, E., Baker, T. R., Lloyd, J., Lopez-Gonzalez, G., Monteagudo-Mendoza, A., Malhi, Y., Lewis, S. L., Viçozque Martinez, R., Alexiades, M., Alvarez-Dívila, E., Alvarez-Loayza, P., Andrade, A., Aragão, L. E. O. C., Araujo-Murakami, A., Arets, E. J. M. M., Arroyo, L., Aymard, G. A., Bink, O. S., Baraloto, C., Barroso, J., Bonal, D., Boot, R. G. A., Camargo, J. L. C., Castilho, C. V., Chama, V., Chao, K. J., Chave, J., Comiskey, J. A., Valverde, F. C., da Costa, L., de Oliveira, E. A., Di Fiore, A., Erwin, T. L., Fauset, S., Forsthofer, M., Galbraith, D. R., Grahame, E. S.,
- 910 Groot, N., Higuchi, B., Higuchi, N., Honorio Coronado, E. N., Keeling, H., Killeen, T. J., Laurance, W. F., Laurance, S., Licona, J., Magnusson, W. E., Marimon, B. S., Marimon-Junior, B. H., Mendoza, C., Neill, D. A., Nogueira, E. M., Nogueira, P., Pallqui Camacho, N. C., Parada, A., Pardo-Molina, G., Peacock, J., Peña-Claros, M., Pickavance, G. C., Pitman, N. C. A., Poorter, L., Prieto, A., Quesada, C. A., Ramírez, F., Ramírez-Angulo, H., Restrepo, Z., Roopsind, A., Rudas, A., Salomão, R. P., Schwarz, M., Silva, N., Silva-Espejo, J. E., Silveira, M., Stropp, J., Talbot, J., ter Steege, H., Teran-Aguilar,
- 915 J., Terborgh, J., Thomas-Caesar, R., Toledo, M., Torello-Raventos, M., Umetsu, K., van der Heijden, G. M. F., van der Hout, P., Guimarães Vieira, I. C., Vieira, S. A., Vilanova, E., Vos, V. A., Zagt, R. J., Alarcon, A., Amaral, I., Camargo, P. P. B., Brown, I. F., Blanc, L., Burban, B., Cardozo, N., Engel, J., et al.: Carbon uptake by mature Amazon forests has mitigated Amazon nations' carbon emissions, *Carbon Balance Manag.*, 12(1), 1–9, doi:10.1186/s13021-016-0069-2, 2017.
- Poorter, L.: The relationships of wood-, gas- and water fractions of tree stems to performance and life history variation in
- 920 tropical trees, *Ann. Bot.*, 102(3), 367–375, doi:10.1093/aob/mcn103, 2008.
- Quesada, C. A., Lloyd, J., Schwarz, M., Baker, T. R., Phillips, O. L., Patiño, S., Czimczik, C., Hodnett, M. G., Herrera, R., Arneeth, A., Lloyd, G., Malhi, Y., Dezzio, N., Luizão, F. J., Santos, A. J. B., Schmerler, J., Arroyo, L., Silveira, M., Priante Filho, N., Jimenez, E. M., Paiva, R., Vieira, I., Neill, D. A., Silva, N., Peñuela, M. C., Monteagudo, A., Vásquez, R., Prieto, A., Rudas, A., Almeida, S., Higuchi, N., Lezama, A. T., López-González, G., Peacock, J., Fyllas, N. M., Alvarez Dávila, E.,
- 925 Erwin, T., Di Fiore, A., Chao, K. J., Honorio, E., Killeen, T., Peña Cruz, A., Pitman, N., Núñez Vargas, P., Salomão, R., Terborgh, J. and Ramírez, H.: Regional and large-scale patterns in Amazon forest structure and function are mediated by variations in soil physical and chemical properties, *Biogeosciences Discuss.*, 6(2), 3993–4057, doi:10.5194/bg-d-6-3993-2009, 2009.
- Quesada, C. A., Phillips, O. L., Schwarz, M., Czimczik, C. I., Baker, T. R., Patiño, S., Fyllas, N. M., Hodnett, M. G., Herrera,
- 930 R., Almeida, S., Alvarez Dávila, E., Arneeth, A., Arroyo, L., Chao, K. J., Dezzio, N., Erwin, T., Di Fiore, A., Higuchi, N., Honorio Coronado, E., Jimenez, E. M., Killeen, T., Lezama, A. T., Lloyd, G., López-González, G., Luizão, F. J., Malhi, Y., Monteagudo, A., Neill, D. A., Núñez Vargas, P., Paiva, R., Peacock, J., Peñuela, M. C., Peña Cruz, A., Pitman, N., Priante Filho, N., Prieto, A., Ramírez, H., Rudas, A., Salomão, R., Santos, A. J. B., Schmerler, J., Silva, N., Silveira, M., Vásquez, R., Vieira, I., Terborgh, J. and Lloyd, J.: Basin-wide variations in Amazon forest structure and function are mediated by both soils
- 935 and climate, *Biogeosciences*, 9(6), 2203–2246, doi:10.5194/bg-9-2203-2012, 2012.
- Rammig, A., Jupp, T., Thonicke, K., Tietjen, B., Heinke, J., Ostberg, S., Lucht, W., Cramer, W. and Cox, P.: Estimating the risk of Amazonian forest dieback, *New Phytol.*, 187(3), 694–706, doi:10.1111/j.1469-8137.2010.03318.x, 2010.



- Reich, P. B. and Borchert, R.: Phenology and ecophysiology of the tropical tree *Tabebuia neochrysantha* (Bignoniaceae) (Guanacaste, Costa Rica)., *Ecology*, 63(2), 294–299, doi:10.2307/1938945, 1982.
- 940 Restrepo-Coupe, N., da Rocha, H. R., Hutrya, L. R., da Araujo, A. C., Borma, L. S., Christoffersen, B., Cabral, O. M. R., de Camargo, P. B., Cardoso, F. L., da Costa, A. C. L., Fitzjarrald, D. R., Goulden, M. L., Kruijt, B., Maia, J. M. F., Malhi, Y. S., Manzi, A. O., Miller, S. D., Nobre, A. D., von Randow, C., Sá, L. D. A., Sakai, R. K., Tota, J., Wofsy, S. C., Zanchi, F. B. and Saleska, S. R.: What drives the seasonality of photosynthesis across the Amazon basin? A cross-site analysis of eddy flux tower measurements from the Brasil flux network, *Agric. For. Meteorol.*, 182–183, 128–144, 945 doi:10.1016/j.agrformet.2013.04.031, 2013.
- Rice, A. H., Hammond, E. P., Saleska, S. R., Hutrya, L. R., Palace, M. W., Keller, M. M., de Camargo, P. B., Portilho, K., Marques, D. and Wofsy, S. C.: LBA-ECO CD-10 Forest Litter Data for km 67 Tower Site, Tapajos National Forest, ORNL Distrib. Act. Arch. Cent., doi:10.3334/ORNLDAAC/862, 2008.
- Rifai, S. W., Girardin, C. A. J., Berenguer, E., Del Aguila-Pasquel, J., Dahlsjö, C. A. L., Doughty, C. E., Jeffery, K. J., Moore, 950 S., Oliveras, I., Riutta, T., Rowland, L. M., Murakami, A. A., Addo-Danso, S. D., Brando, P., Burton, C., Ondo, F. E., Duah-Gyamfi, A., Amézquita, F. F., Freitag, R., Pacha, F. H., Huasco, W. H., Ibrahim, F., Mbou, A. T., Mihindou, V. M., Peixoto, K. S., Rocha, W., Rossi, L. C., Seixas, M., Silva-Espejo, J. E., Abernethy, K. A., Adu-Bredu, S., Barlow, J., da Costa, A. C. L., Marimon, B. S., Marimon-Junior, B. H., Meir, P., Metcalfe, D. B., Phillips, O. L., White, L. J. T. and Malhi, Y.: ENSO Drives interannual variation of forest woody growth across the tropics., *Philos. Trans. R. Soc. Lond. B. Biol. Sci.*, 373(1760), 955 20170410, doi:10.1098/rstb.2017.0410, 2018.
- Roberts, D. A., Nelson, B. W., Adams, J. B. and Palmer, F.: Spectral changes with leaf aging in Amazon caatinga, *Trees - Struct. Funct.*, 12(6), 315–325, doi:10.1007/s004680050157, 1998.
- Roberts, J., Cabral, O. M. R. and Aguiar, L. F. De: Stomatal and Boundary-Layer Conductances in an Amazonian terra Firme Rain Forest, *Br. Ecol. Soc.*, 27(1), 336–353, doi:10.2307/2403590, 1990.
- 960 Rohatgi, A.: WebPlotDigitizer, [online] Available from: <https://automeris.io/WebPlotDigitize>, 2018.
- Saatchi, S., Asefi-Najafabady, S., Malhi, Y., Aragao, L. E. O. C., Anderson, L. O., Myneni, R. B. and Nemani, R.: Persistent effects of a severe drought on Amazonian forest canopy, *Proc. Natl. Acad. Sci.*, 110(2), 565–570, doi:10.1073/pnas.1204651110, 2013.
- Saleska, S. R., Didan, K., Huete, A. R. and da Rocha, H. R.: Amazon Forests Green-Up During 2005 Drought, *Science* (80- 965), 318(5850), 612–612, doi:10.1126/science.1146663, 2007.
- Samanta, A., Ganguly, S., Hashimoto, H., Devadiga, S., Vermote, E., Knyazikhin, Y., Nemani, R. R. and Myneni, R. B.: Amazon forests did not green-up during the 2005 drought, *Geophys. Res. Lett.*, 37(5), doi:10.1029/2009GL042154, 2010.
- Sanches, L., Valentini, C. M. A., Pinto Júnior, O. B., Nogueira, J. de S., Vourlitis, G. L., Biudes, M. S., da Silva, C. J., Bambi, P. and Lobo, F. de A.: Seasonal and interannual litter dynamics of a tropical semideciduous forest of the southern Amazon 970 Basin, Brazil, *J. Geophys. Res. Biogeosciences*, 113(4), G04007, doi:10.1029/2007JG000593, 2008.
- Santos, V. A. H. F. dos, Ferreira, M. J., Rodrigues, J. V. F. C., Garcia, M. N., Ceron, J. V. B., Nelson, B. W. and Saleska, S.



- R.: Causes of reduced leaf-level photosynthesis during strong El Niño drought in a Central Amazon forest., 2018.
- Schaik, E. van, Kooreman, M., Stammes, P., Tuinder, O. N., Sanders, A. F., Verstraeten, W., Lang, R., Cacciari, A., Joiner, J. and Peters, W.: Improved SIFTER v2 algorithm for long-term GOME-2A satellite retrievals of fluorescence with a correction
975 for instrument degradation, *Atmos. Meas. Tech. Discuss.*, (January), 1–33, doi:10.5194/amt-2019-384, 2020.
- Schessl, M., Silva, W. L. Da and Gottsberger, G.: Effects of fragmentation on forest structure and litter dynamics in Atlantic rainforest in Pernambuco, Brazil, *Flora Morphol. Distrib. Funct. Ecol. Plants*, 203(3), 215–228, doi:10.1016/j.flora.2007.03.004, 2008.
- Selva, E. C., Couto, E. G., Johnson, M. S. and Lehmann, J.: Litterfall production and fluvial export in headwater catchments
980 of the southern Amazon, *J. Trop. Ecol.*, 23(3), 329–335, doi:10.1017/S0266467406003956, 2007.
- Sizer, N. C., Tanner, E. V. J. and Kossmann Ferraz, I. D.: Edge effects on litterfall mass and nutrient concentrations in forest fragments in central Amazonia, *J. Trop. Ecol.*, 16(6), 853–863, doi:10.1017/S0266467400001760, 2000.
- Sombroek, W.: Spatial and Temporal Patterns of Amazon Rainfall, *AMBIO A J. Hum. Environ.*, 30(7), 388–396, doi:10.1579/0044-7447-30.7.388, 2001.
- 985 Soong, J. L., Janssens, I. A., Grau, O., Margalef, O., Stahl, C., Van Langenhove, L., Urbina, I., Chave, J., Dourdain, A., Ferry, B., Freycon, V., Herault, B., Sardans, J., Peñuelas, J. and Verbruggen, E.: Soil properties explain tree growth and mortality, but not biomass, across phosphorus-depleted tropical forests, *Sci. Rep.*, 10(1), 1–13, doi:10.1038/s41598-020-58913-8, 2020.
- Stahl, C., Burban, B., Bompoy, F., Jolin, Z. B., Sermage, J. and Bonal, D.: Seasonal variation in atmospheric relative humidity contributes to explaining seasonal variation in trunk circumference of tropical rain-forest trees in French Guiana, *J. Trop. Ecol.*,
990 26(4), 393–405, doi:10.1017/S0266467410000155, 2010.
- Stahl, C., Burban, B., Wagner, F., Goret, J.-Y., Bompoy, F. and Bonal, D.: Influence of Seasonal Variations in Soil Water Availability on Gas Exchange of Tropical Canopy Trees, *Biotropica*, 45(2), 155–164, doi:10.1111/j.1744-7429.2012.00902.x, 2013.
- Thomas, R. S.: Forest Productivity and Resource Availability in Lowland Tropical Forests of Guyana by Thesis submitted for
995 the degree of Doctor of Philosophy of the University of London and for the Diploma of Imperial College, , (June), 1999.
- Vasconcelos, S. S., Zarin, D. J., Araújo, M. M. and Miranda, I. de S.: Aboveground net primary productivity in tropical forest regrowth increases following wetter dry-seasons, *For. Ecol. Manage.*, 276, 82–87, doi:10.1016/j.foreco.2012.03.034, 2012.
- Veneklaas, E. J.: Litterfall and Nutrient Fluxes in Two Montane Tropical Rain Forests , Colombia, *J. Trop. Ecol.*, 7(3), 319–336, 1991.
- 1000 Wagner, F., Rossi, V., Stahl, C., Bonal, D. and Héroult, B.: Asynchronism in leaf and wood production in tropical forests: A study combining satellite and ground-based measurements, *Biogeosciences*, 10(11), 7307–7321, doi:10.5194/bg-10-7307-2013, 2013.
- Whigham, D. F., Olmsted, I., Cano, E. C. and Harmon, M. E.: The Impact of Hurricane Gilbert on Trees , Litterfall , and Woody Debris in a Dry Tropical Forest in the Northeastern Yucatan Peninsula, *Biotropica*, 23(4), 434–441, 1991.
- 1005 Wieder, K. R. and Wright, S. J.: Tropical Forest Litter Dinamic and dry Irrigation on Barro Colorado Island, Panama, *Ecology*,



- 76(6), 1971–1979, 2001.
- Wolfe, B. T., Sperry, J. S. and Kursar, T. A.: Does leaf shedding protect stems from cavitation during seasonal droughts? A test of the hydraulic fuse hypothesis, *New Phytol.*, 212(4), 1007–1018, doi:10.1111/nph.14087, 2016.
- Worbes, M.: Annual growth rings, rainfall-dependent growth and long-term growth patterns of tropical trees from the Caparo Forest Reserve in Venezuela, *J. Ecol.*, 87(3), 391–403, doi:10.1046/j.1365-2745.1999.00361.x, 1999.
- 1010 Xu, L., Samanta, A., Costa, M. H., Ganguly, S., Nemani, R. R. and Myneni, R. B.: Widespread decline in greenness of Amazonian vegetation due to the 2010 drought, *Geophys. Res. Lett.*, 38(7), 2–5, doi:10.1029/2011GL046824, 2011.
- Yang, J., Tian, H., Pan, S., Chen, G., Zhang, B. and Dangal, S.: Amazon drought and forest response: Largely reduced forest photosynthesis but slightly increased canopy greenness during the extreme drought of 2015/2016, *Glob. Chang. Biol.*, 24(5), 1015 1919–1934, doi:10.1111/gcb.14056, 2018.
- Zhu, Z., Bi, J., Pan, Y., Ganguly, S., Anav, A., Xu, L., Samanta, A., Piao, S., Nemani, R. R. and Myneni, R. B.: Global data sets of vegetation leaf area index (LAI)_{3g} and fraction of photosynthetically active radiation (FPAR)_{3g} derived from global inventory modeling and mapping studies (GIMMS) normalized difference vegetation index (NDVI_{3G}) for the period 1981 to 2, *Remote Sens.*, 5(2), 927–948, doi:10.3390/rs5020927, 2013.
- 1020